Zooplankton biomass, size structure, and associated metabolic fluxes with focus on its roles at the chlorophyll maximum layer during the plankton-contaminant MERITE-HIPPOCAMPE cruise

Pamela Fierro-González, Marc Pagano, Loïc Guilloux, Nouha Makhlouf, Marc Tedetti, François Carlotti

Zooplankton biomass, size structure, and associated metabolic fluxes with focus on its roles at the chlorophyll maximum layer during the plankton-contaminant MERITE-HIPPOCAMPE cruise

Pamela Fierro-González [a], Marc Pagano [a], Loïc Guilloux [a], Nouha Makhlouf [a,b], Marc Tedetti [a], François Carlotti [a,*]

[a] Aix Marseille Univ, Université de Toulon, CNRS, IRD, MIO UM 110, 13288 Marseille, France
[b] Université de Carthage Faculté des Sciences de Bizerte, Zarzouna 7021, Tunisia

ARTICLE INFO

Keywords:
Zooplankton biomass
Zooplankton structure size and taxonomic groups
Metabolic fluxes
Vertical versus horizontal sampling
Mediterranean North-South transect

ABSTRACT

Recent studies have demonstrated that plankton can be a key pathway for the uptake and transfer of contaminants entering the marine environment up to top predators.

The plankton-contaminant MERITE-HIPPOCAMPE cruise was devoted to quantifying contaminants in water and the whole plankton size range (10 size fractions) at 10 stations along a north-south transect in the western Mediterranean Sea from the French to the Tunisian coasts through the Provençal and Algerian basins. Pumping and filtering devices and net sampling have been used for collecting very high amounts of small particles and planktonic organisms in the chlorophyll maximum layer (CML). The present paper characterizes the zooplankton components for which the contaminant measurements were carried out. At each station, a horizontal towed Hydro-Bios net with a 60 µm mesh-size net was used to discriminate 5 size-fractions from 60 µm to a few mm. For each size-fraction, one part of the sample was used for dry weight measurements and the other one for estimating the contribution to biomass of detritus, phytoplankton, and among zooplankton of the major taxonomic groups based on the imagery tools ZOOSCAN and FLOWCAM. In each zooplankton size fraction, metabolic rates were calculated from the size spectrum to estimate trophic and excretion fluxes flowing through this fraction. These observations were compared to a similar analysis of tows in the upper layer (vertical) and the surface layer (horizontal).

The total sampled biomass concentration at the CML was higher than in the water column (COL) and much higher than at the surface (SURF) in most of the stations, but in the CML and COL a substantial contribution was due to detritus mostly concentrated in the smallest size-fractions (60–200 µm and 200–500 µm). Absolute values of zooplankton biomass show neither a clear spatial pattern nor a significant difference between strata. The CML layer was dominated by copepods similarly to COL and SURF, but presented a higher contribution of nauplii and a near absence of appendicularians. At some stations, crustaceans and gelatinous plankton could be important contributors to CML. The zooplankton biomass composition of the two smallest fractions (<500 µm) was dominated by nauplii, small copepods and, occasionally, by small miscellaneous organisms (mostly pteropodes). In contrast, clear differences between stations appeared for the largest fractions (>500 µm) due to large crustaceans, gelatinous organisms, and chaetognaths. These changes in biomass composition according to size fractions suggest a progressive trophic shift from dominant herbivory in the smallest fractions to more contrasted trophic structure (including carnivory) in the largest fractions.

The daily carbon demand and the N and P excretion of zooplankton were on average higher at the CML but with no significant difference with COL. The zooplankton grazing represented 2.7 to 22.7 % of the phytoplankton stock per day, whereas its excretion represented a daily N and P recycling compared to dissolved inorganic nitrogen and phosphorus stocks ranging respectively from 0.2 to 19 % and from 0 to 21 %. This information should help in the interpretation of the content of various contaminants in zooplankton fractions.

1. Introduction

Organic and metallic contamination levels have been monitored at alarming levels in large marine vertebrates (fish, mammals) in many regions and for several decades (Das et al., 2002; Van der Oost et al., 2003; Weijs et al., 2014; Khairy et al., 2021). However, it is only recently that measurements of contaminants have become available in the surrounding environment and in the prey of these organisms, and have proven to be necessary for understanding the processes of contaminant accumulation in bottom-up food webs (Weijs et al., 2014). Several recent studies have demonstrated that plankton can be a key pathway for the uptake and transfer of contaminants entering the marine environment, playing a potential ecological role as the biological pump of contaminants (Tiano et al., 2014; Strady et al., 2015; Chouvelon et al., 2019). Trophic transfer models of contaminants underline the need for a better evaluation of transfer processes, particularly by trophic interactions, with a prerequisite being the availability of consistent data on contaminant content in successive trophic levels (Alekseenko et al., 2018). However, such studies are most often limited to a segment of the planktonic food-web for methodological reasons; to accurately measure these contaminant levels, large sample volumes are required and must enable distinction between different planktonic trophic levels. Pumping and filtering devices have been widely developed for collecting very high amounts of small particles and planktonic organisms smaller than microplankton (phyto- and zoo-) based on size-fractionation (e.g. Wen et al., 2018). A recent integrated study in the Gulf of Lion dedicated to investigating sardine and anchovy contamination (COSTAS) has extended this size fraction approach to the meso- and macro-zooplankton categories of net-collected organisms (Tiano et al., 2014; Chouvelon et al., 2019), giving an adequate fractional resolution for tracing contaminants in the planktonic network.

It is therefore important to further develop approaches that collect large plankton biomass in the same water bodies and that sort these biomasses by size fractions across the whole planktonic size range. The aim of the MERMEX MERITE program was to improve and test different approaches of collection/size fractionation of plankton biomasses in coastal areas (Bay of Toulon, Bay of Marseille, Gulf of Gabès), before defining a global protocol to be used along a north-south transect in the Mediterranean Sea, from the French coast to the Tunisian coast, passing offshore of Corsica and Sardinia: the MERITE HIPPOCAMPE campaign (Tedetti et al., 2023). The campaign consisted of sampling large volumes of water and seston including plankton for measuring a large spectrum of organic and metallic contaminants (see details of survey strategy in Tedetti et al., 2023). For the 10 stations investigated, the samples were collected in one common layer in the water column, the chlorophyll maximum layer (CML), assumed to be the layer with the highest concentrations of plankton (mainly phytoplankton, but supposed to be attractive for zooplankton). Sampling was done using pumping systems (McLane pumps) and a horizontal towed Hydro-Bios net with 60 µm mesh-size net allowing discrimination up to 5 size-fractions between 0.2 and 60 µm and 5 size-fractions between 60 µm and a few mm (see details of methodology in Tedetti et al., 2023).

The aim of the present paper is to characterize the zooplankton components (from 60 µm to a few mm) in the different fractions of the samples collected at the CML of each station for which the contaminant measurements were carried out. For each size-fraction, the contribution to the biomass of detritus, of phytoplankton, and among zooplankton of the major taxonomic groups has been quantified. Metabolic rates calculated from the size spectrum of each zooplanktonic size fraction enable estimation of trophic and excretion fluxes flowing through this size fraction. To assess whether the contribution of taxonomic groups to the zooplankton biomass in the CML reveals a particular niche or not, it is compared to similar analyses carried out on vertical features in the epipelagic zone (200 m depth or bottom to surface).

2. Material and methods

2.1. Study area and sampling strategy

The MERITE-HIPPOCAMPE cruise was carried out between 13 April and 14 May 2019, during the spring bloom, along a north-south transect in the western Mediterranean Sea, from the French coast (Toulon, Marseille) to the Tunisian coast (Gulf of Gabès) aboard the French Research Vessel *Antea* (Fig. 1). Ten stations were sampled during 2 legs. Five stations (St02, St04, St03, St10, and St11) from Toulon to Tunis during Leg 1 (second half of April), and five other stations (St15, St17, St19, St09, and St01) from Tunis to the south of the Gulf of Gabès and then on the way back to Toulon - La Seyne, during Leg 2 (first half of May). For each station, the date of sampling, the geographical position, the station depth, and the depth of different samples (CTD and net tows explained below) are presented in Table 1.

2.2. Environmental data

At each station, an oceanographic carousel equipped with a CTD Seabird SBE 911plus to measure the hydrological variables (temperature, density and salinity) was deployed down to 250 m for open-sea stations or near the bottom for shallower stations (see Table 1). In addition, the CTD was coupled with several sensors including chlorophyll-a fluorescence (Chla; Aqua Tracka, Chelsea ctg).

2.3. Zooplankton sampling and sample processing

Zooplankton samples were obtained using three different types of nets for different strata in the water column (Table 2). A Multiple Plankton Sampler (Midi type, Hydro-Bios) with a square aperture surface of 0.25 m^2 towed at a constant speed of around 2 knots was used for sampling horizontally at the depth of the CML (see sampling depth for each station in Table 1), with five successive shut-off nets of 60 µm mesh-size, each of them filtering a water volume of around 50 to 80 m^3 (estimated by automatic detection with internal and external flowmeters, and according to plankton load before clogging). A Manta net was used for surface sampling, with a rectangular aperture of 0.7 × 0.4 m, and a 60 µm mesh-size net, towed at a constant speed of 2 knots for 10

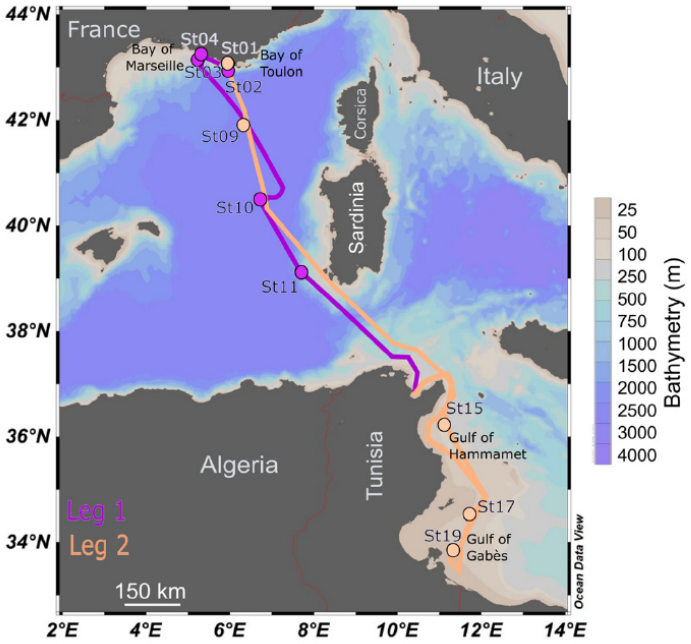

Fig. 1. Map of sampled stations during the two legs of the MERITE-HIPPOCAMPE cruise (13 April–14 May 2019) on board the RV *Antea*.

min.

A steel frame with three circles (triple-net), each with a 60 cm diameter opening, was towed vertically at a constant speed of 0.7 m/s through the water column from 200 m depth (or near the bottom) to the surface (see depth of vertical net lines for each station in Table 1). Three different mesh size nets - 60, 120 and 200 µm - were attached to the triple-net. The sample collected by the 120 µm net was not analyzed in this study, since the samples collected with the 60 and 200 µm nets provided a complete coverage of the zooplankton size spectrum. Moreover, the community observed within the 60 µm vertical net can be compared with the one collected at the DCM with the Hydrobios net.

For further zooplankton analysis (biomass imagery, and microscopy), the samples from the different nets were fractionated using stainless-steel sieves of different mesh-sizes. The fractionation scheme slightly differed between nets due to different scientific objectives (Table 2). The samples from Hydro-Bios were fractionated on board through a column of into five size fractions (60–200, 200–500, 500–1000, 1000–2000 and >2000 µm). These size-fractions were defined for studying contaminants and therefore large volumes (between 300 and 2400 m^3) were filtered in order to get enough plankton in all fractions to measure contaminants and other parameters (Tedetti et al., 2023). Around 10 % of each of these fractions were kept for zooplankton analysis (NB: however, at a few stations, not enough plankton material was recovered for the largest fractions, i.e. stations 04, 17 and 19). Then, they were split into two sub-samples: one kept at −20 °C for further dry biomass weighing (mg DW m^{-3}), and the other one preserved in 4 % borax-buffered formalin for imagery treatment. The protocol of fractions for Manta nets was imposed for a comparison with a classical 300 µm mesh-size Manta net deployed in parallel (EU-MSFD protocols, results not presented in this paper). Thus, two fractions (below and above 300 µm) were considered for weighing, and then sub-fractionating was done for imagery analysis, allowing comparisons with Hydro-Bios samples. For the 60 µm mesh-size vertical net, only the lowest three size fractions common with those of Hydro-Bios were considered (because the plankton content was generally low). However, larger fractions were observed in the 200 µm mesh size net. Sub-samples of each fraction from the Manta net and vertical nets were preserved in a similar way as for Hydro-Bios samples and for similar analysis (see Table 2).

2.4. Zooplankton imagery treatment

Sample fractions below 500 µm were processed using a FlowCAM (see Table 2; Yokogawa Fluid Imaging Technologies Inc. Series VS-IV benchtop model (Sieracki et al., 1998). The other fractions were treated using a ZOOSCAN (Gorsky et al., 2010). For both imagery sample treatments (FlowCam and Zooscan), the analyses were done following the protocol described by Feliú et al. (2020). Distinct biological components and particles were differentiated: microalgae (eukaryotic microalgae and prokaryotic cyanobacteria) and non-living detritus material (marine snow, aggregates), and several living taxonomic groups of zooplankton: nauplii, copepods, crustaceans, appendicularians, gelatinous organisms, chaetognaths, and other diverse zooplankton groups (including molluscs, polychaetes, and rare protozoans) gathered in one group named 'miscellaneous' below. For each category, the abundance of organisms (ind m^{-3}) or particles (nb m^{-3}), and their area (mm^2) and biovolume (mm^3) were provided.

2.5. Biomass measurements and derived carbon demand, respiration, and excretion by zooplankton

In the laboratory, dry-weight biomasses were determined after drying samples on pre-weighed GF/F filters (60 °C, 24 h) and then re-weighed with a microbalance (Mettler, precision 0.1 mg) according to the protocol established by Lovegrove (1966). The contributions of zooplankton, detritus, and microalgae components to the total weighed biomass were estimated by using for zooplankton individuals the relationships from Lehette and Hernández-León (2009) between body-area and body-weight, and for detritus and microalgae particles the biovolume-weight relationships from Alldredge (1998). Zooplankton biomass was converted into carbon assuming the carbon/dry-weight ratios given by Gorsky et al. (1988) for Mediterranean zooplankton taxa.

The zooplankton carbon demand (ZCD, in mg C m^{-3} d^{-1}), respiration rates and ammonium and phosphorus excretion rates (both in µmol L^{-1} d^{-1}) were computed following the protocol described by Feliú et al. (2020), and based on allometric relationships to individual body-weight.

2.6. Data analysis

A principal component analysis (PCA) was performed on the environmental parameters, including temperature, density, salinity, and chlorophyll concentration (from in situ fluorescence measurements). For the spatial patterns of zooplankton communities, a taxonomic group–station matrix was created using the biomass values; this was square-root transformed to estimate Bray–Curtis similarity distances. The similarity matrix was then ordinated using non-metric multidimensional scaling (NMDS). These two analyses were performed using PRIMER v7 software (Anderson et al., 2008).

We tested for significant differences in biomasses (total, size fractions, and taxa groups) using Student's *t*-tests between samples of the two vertical nets of the whole water column with mesh-size of 60 and 200 µm, and between samples of the whole water column (COL-60) and from CML. Data were first verified for normality using the Kolmogrow-Smirnov test and for homogeneity of variance using a Fisher F-test. Mann Whitney *U* test was used to compare the grazing pressure of zooplankton between areas.

Below, CML, SURF, COL refer to the three different strata sampled with nets, respectively, the chlorophyll maximum layer, the surface layer, and the integrated water column layer. COL-60 and COL-200 refer to the mesh-size nets of 60 and 200 µm used for the integrated water column tow.

Table 1
Stations sampled during the MERITE-HIPPOCAMPE cruise: date, geographical position, bottom depths, maximum depths of CTD cast and of vertical triple net tow, and depth of horizontal Hydro-Bios net tow.

Station	Date	Latitude (N)	Longitude (E)	Bottom depth (m)	Depth of CTD cast (m)	Depth Triple vertical net (m)	Depth Hydro-Bios net (m)
st01	11-05-2019	43°04.398	5°58.838	91	88	80	24
st02	15-04-2019	42°56.009	5°57.739	1770	250	210	31
st03	20-04-2019	43°08.823	5°14.199	95	100	85	55
st04	16-04-2019	43°14.876	5°19.001	58	50	48	35
st09	09-05-2019	41°54.661	6°20.163	2575	250	200	20
st10	24-04-2019	40°23.251	7°11.034	2791	250	180	40
st11	25-04-2019	39°08.193	7°40.382	1378	250	182	35
st15	30-04-2019	36°12.164	11°08.057	100	95	80	68
st17	02-05-2019	34°30.118	11°43.593	48	48	39	37
st19	03-05-2019	33°51.226	11°20.165	50	50	42	39

3. Results

3.1. Spatial pattern of environmental variables

The first axis of the principal component analysis (PCA) on environmental variables (79.6 % of variability) correlated with changes of temperature and salinity separating the stations located north (St01 to St09) and south (St10 to St19) of the Balearic front. Stations St10 and St11 have intermediate positions with their temperature and salinity in COL (both stations) and CML (St10 only) being close to those of the northern stations, whereas temperature and salinity are close to those of the southern stations for SURF and CML of St11. The second axis (15.6 %) is correlated with chlorophyll and differentiates CML, SURF and COL values, more or less strong according to the stations, with the highest difference at St09 (Fig. 2).

In general, the temperature and salinity profiles did not show strong stratification of the water column during the cruise (see detailed profiles of oceanographic and biological variables presented in Fig. 4). Temperature values ranged from 14 to 17.8 °C at the surface (and very close values at CML), with the highest values recorded in the Gulf of Gabès.

In the southern basin, the coastal stations of Tunisia (St15, 17, and 19) and stations 10 and 11 presented salinity profiles below 38 (with the exception of St10, which had values higher than 38 below 79 m depth), whereas the northern stations were above 38 (with the exception of the first two meters of surface at St03). St09 presented the highest salinity in the northern basin and showed a strong contrast with St10, the nearest station in the southern basin. In general, the Chla vertical distribution presented a well-pronounced maximum at the CML, located near or above the bottom for most of the coastal stations (St19, 17, 15, and 03), or fluctuating in a more spread profile due to mixing (St01 and 04), St02 showing a typical Chl*a* peak at mid-water depth. Among the offshore stations, St09 presented the highest values of the campaign, distributed in a broad surface mixed layer with a maximum value at 20 m, whereas St10 and St11 presented a CML at 40–45 m although more prominent at St10.

3.2. Spatial patterns of plankton and detritus biomasses

NMDS analysis of the percentage of zooplankton taxa biomass reveals differences in compositions among strata for all stations. Some stations (St01, 02, 09, and 19) showed short distances between values of the three strata in the NMDS plot (Fig. 2b) and this corresponded to only small differences, among these strata, in biomass composition with high dominance of the copepods (Fig. 3a–d). Inversely, in the other stations (St03, 04, 10, 11, 15, and 17), wide differences between values of the three strata in the NMDS plot are related to the dominance of other taxonomic groups in one or two layers, e.g. importance of crustaceans at the CML at St03, 04, 11 and 15, or in SURF at St10 and 17, or dominance of gelatinous in COL at St15. From NMDS no clear regional patterns in zooplankton biomass composition appear, nor evident differences between coastal and off-shore stations, which would indicate for each station a local influence of hydrography and short-term meteorology on the biological biomass distribution.

The total sampled biomass was often higher at the CML than in COL-60 (St01, 02, 04, 09, 11, and 17), but in some cases, it was equivalent (St10, 15 and 17) or even lower (St03) and there was no significant difference between the mean values of the two strata (*t*-test; $p = 0.12$). Both strata showed higher values at the coastal stations (St01, 04, 17 and 19) than at the oceanic stations (St02, 09, 10, 11). SURF showed total biomass generally much lower (Fig. 3e–h) and significantly different than those recorded in COL or CML (paired *t*-test, $p = 0.035$ and 0.020, respectively). Detritus was almost absent in SURF (Fig. 3f) but represented a high proportion of the total sampled biomass in COL and CML, particularly in the shallowest southern (St17 and 19) and northern stations (St04 at the CML) (Fig. 3e and g). Microalgae were collected at the CML of almost all stations but always with very low biomass compared to detritus and zooplankton, except at some coastal stations (St01, 04, 17, and 19). They were very low in most COL samples, except at St17 and were almost absent in SURF. The absolute values of zooplankton biomass show neither a clear spatial pattern nor a significant difference (paired *t*-test, $p > 0.1$) between the mean values of the three sampled strata (Fig. 3e–h).

The comparison between the two vertical nets, the 60 µm (COL-60) (Fig. 3c and g) and the 200 µm (COL-200) (Fig. 3d and h) mesh-size nets, shows firstly that detritus and microalgae were collected almost exclusively by COL-60. In general, zooplankton biomass was of the same order for COL-60 and COL-200 (paired *t*-test; $p = 0.16$), but with some differences in percentages of taxa. Nauplii, copepods, crustaceans, and miscellaneous presented significant differences between the COL nets (paired *t*-test, $p < 0.05$), whereas no differences appeared for appendicularians, chaetognaths, and gelatinous organisms.

3.3. Zooplankton and detritus biomass in different layers at each station

St01 is a coastal station in the inner Bay of Toulon (Fig. 4a). The water column presents a light thermocline at 10 m and a homogeneous salinity over the 80 m profile. The fluorescence profile presents values of around 0.3 mg Chl*a* m^{-3} at the surface, a maximum of 0.59 mg Chl*a* m^{-3} at around 20 m (CML), and then a regular decrease down to the bottom. CML presents high values of zooplankton biomass (45.8 mg DW m^{-3}), almost twice the COL averaged biomass over 80 m (25.2 mg DW m^{-3}) and SURF biomass (19.7 mg DW m^{-3}). For detritus, the CML biomass is comparable to the COL biomass, whereas SURF biomass is weak. Microalgae were found at the CML. Zooplankton biomass was dominated by copepods and nauplii in the three strata, respectively 96, 92, and 78 % for CML, COL and SURF (Fig. 3a–c), and SURF differed by relatively high biomass of crustaceans and gelatinous organisms.

St02 is offshore of Toulon Bay (Fig. 4b). The water column presents

Table 2
Scheme of treatments of the various size-fractions from the 3 nets used during the MERITE-HIPPOCAMPE cruise.

Net type	Mesh-size (µm)	Size fractions (µm)	Weight	Size fractions (µm)	Imagery treatment
Hydro-Bios	60	>2000	Dry weight	>2000	Zooscan
		1000–2000	Dry weight	1000–2000	Zooscan
		500–1000	Dry weight	500–1000	Zooscan
		200–500	Dry weight	200–500	FlowCam
		60–200	Dry weight	60–200	FlowCam
Triple Vertical	200	>200	Dry weight	>1000	Zooscan
				200–1000	Zooscan
	60	>60	Dry weight	>500	Zooscan
				200–500	FlowCam
				60–200	FlowCam
Manta	60	>300	Dry weight	>1000	Zooscan
				300–1000	Zooscan
		60–300	Dry weight	200–300	FlowCam
				60–200	FlowCam

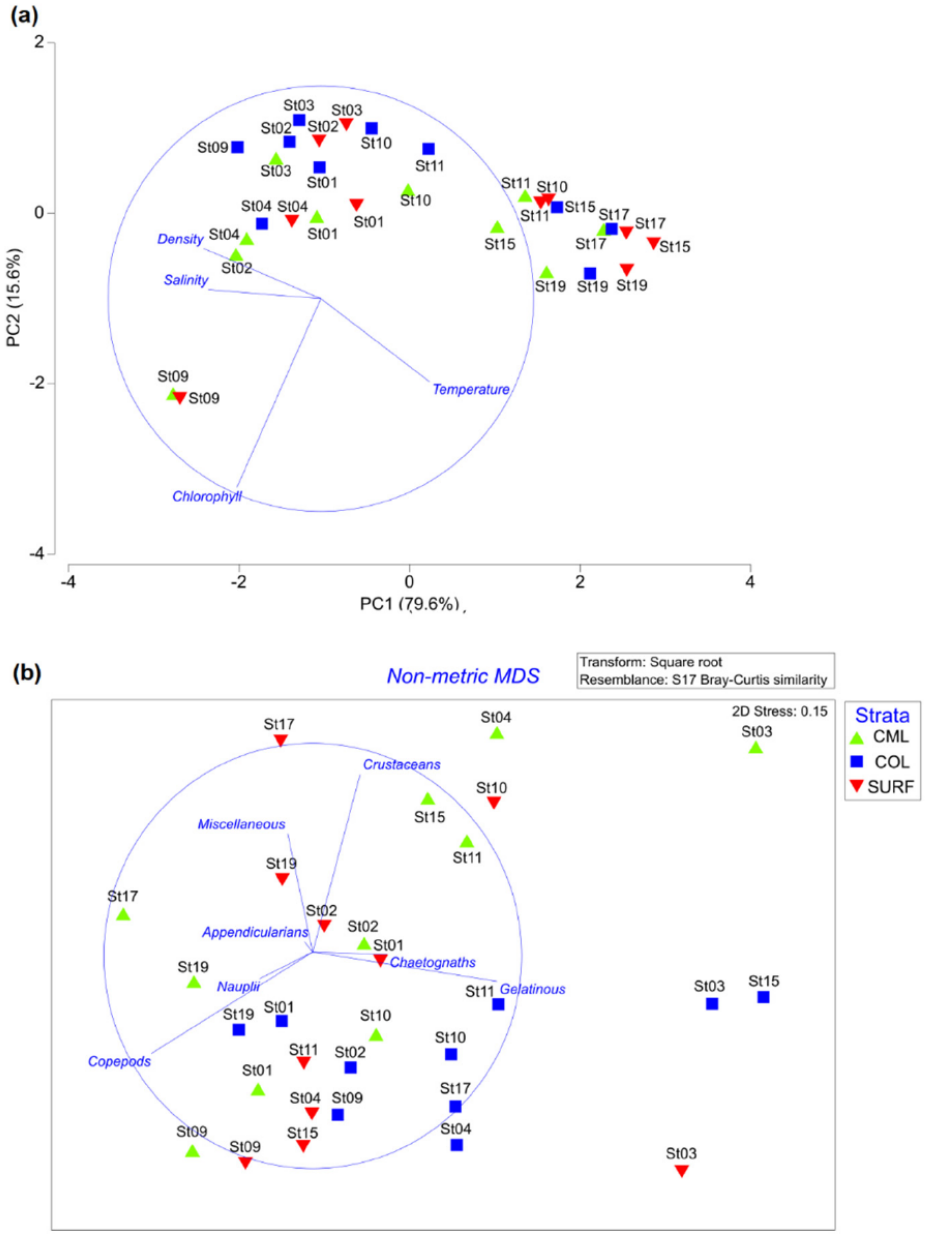

Fig. 2. (a) Principal component analysis (PCA) ordination of four environmental indicators: temperature, salinity, density and chlorophyll, and (b) Nonmetric Multi-Dimensional Scaling (NDMS) on zooplankton taxa relative biomass, for all sampled stations of the MERITE-HIPPOCAMPE cruise. Blue squares: Integrated water column values (COL) from the bottom depth (or 200 m depth) to the surface. Green triangles: values at the chlorophyll maximum layer (CML). Red triangles: values at the surface layer (SURF). (For interpretation of the references to color in this figure legend, the reader is referred to the web version of this article.)

almost homogenous temperature and salinity profiles. The fluorescence profile presents values around 0.2 mg Chl*a* m^{-3} at the surface and a maximum value of 0.93 mg Chla m^{-3} at 32 m (CML). Microalgae were found at CML only. For detritus, CML biomass is comparable to COL biomass (14.2 and 12.6 mg DW m^{-3}, respectively), whereas SURF biomass is weak (2.8 mg DW m^{-3}). The zooplankton biomass was twice as high at CML (10.4 mg DW m^{-3}) than in COL (5.5 mg DW m^{-3}) and three times higher than in SURF (3.5 mg DW m^{-3}). The contribution of zooplankton taxa differed between strata (Fig. 3a–c) with the highest percentage of crustaceans in CML (15 %), compared to SURF and COL (8 and 3 % respectively), and also in the case of appendicularians only present in SURF (10 %).

St03 is situated offshore of Marseille Bay, above the head of the Planier Canyon on the shelf break (Fig. 4c). The water column presents a homogeneous temperature profile, whereas salinity has low values at the surface. The fluorescence profile ranged between 0.08 mg Chla m^{-3} in SURF and 0.39 m^{-3} at CML (52 m). Microalgae were almost absent. The highest zooplankton and detritus biomass values were registered in COL (average ~ 85 m, 35 and 22 mg DW m^{-3}, respectively), and the lowest values in SURF (4.1 and 0.8 mg DW m^{-3}). Zooplankton biomass shows a strong dominance of gelatinous organisms in all strata (42.5 % in CML and 54.2 % in COL) (Fig. 3a–c). Crustaceans represent 30 % of zooplankton biomass in CML but were low in COL (4.6 %) and SURF (0.7 %).

St04 is within the Bay of Marseille (Fig. 4d). The water column presents a homogeneous temperature profile and a shallow halocline at 6 m. The fluorescence profile presents values of 0.6 mg Chla m^{-3} in SURF and a maximum of 0.83 mg Chla m^{-3} at CML (33 m). Higher biomass of detritus and microalgae were observed in the CML (50.5 and 30 mg DW m^{-3}, respectively) compared to SURF and COL. Inversely, zooplankton biomass was higher in COL (29.1 mg DW m^{-3} over the 48 m of the water column) compared to SURF and CML (26.9 and 19.6 mg DW m^{-3}, respectively). The zooplankton biomass was different among strata, characterized by highest contribution of gelatinous organisms and copepods in COL (20.3 and 74 %, respectively), whereas CML was dominated by crustaceans (55 %), and SURF by copepods (93 %) (Fig. 3a–c).

St09 is an offshore station in the north of the North Balearic Thermal Front (Fig. 4e). Both temperature and salinity profiles are homogeneous, although temperature displays a light thermocline at 22 m corresponding to the CML at the bottom of a surface mixed layer. The Chla profile shows high values (1.4 mg Chla m^{-3}) above the CML, and then

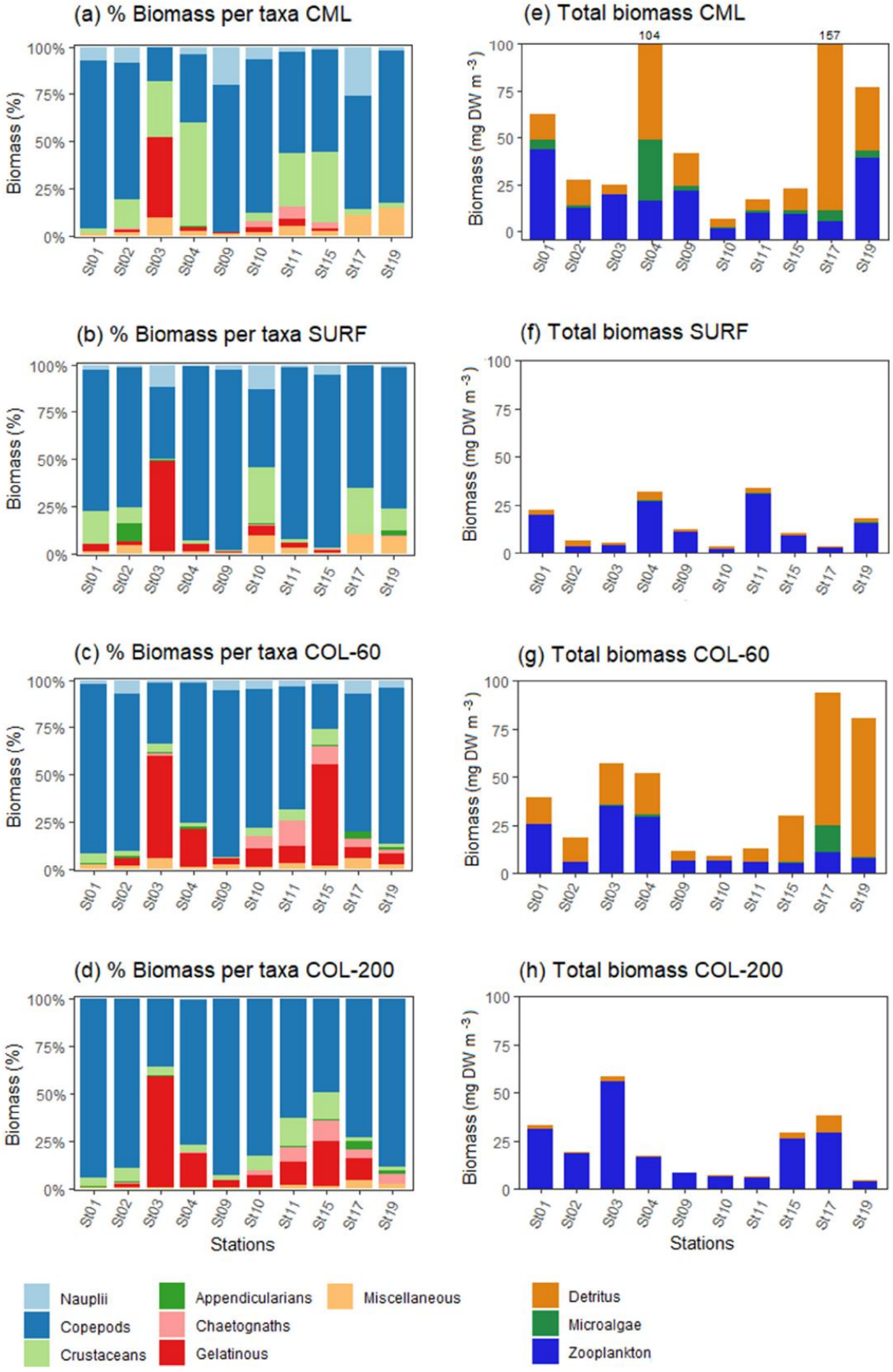

Fig. 3. *Left column*: Cumulated percentages of zooplankton taxa biomasses sampled at each station in the different strata (a) at the Chlorophyll maximum layer (CML), with the 60 µm mesh-size Hydro-Bios nets, (b) at the surface layer (SURF) with the 60 µm mesh-size Manta net, and in the whole water column with a vertical tow (c) of the 60 µm (COL-60) and (d) of the 200 µm (COL-200) mesh-size nets. *Right column*: Total biomass concentration (mg DW m^{-3}) (e) at the Chlorophyll maximum layer (CML), (f) at the surface layer (SURF), and for the integrated water column with (g) net 60 µm (COL-60) and (h) net 200 µm (COL-200). The colored bars, blue, green and orange, represent the cumulated contributions to the total biomass concentrations by zooplankton, microalgae and detritus, respectively. (For interpretation of the references to colo6r in this figure legend, the reader is referred to the web version of this article.)

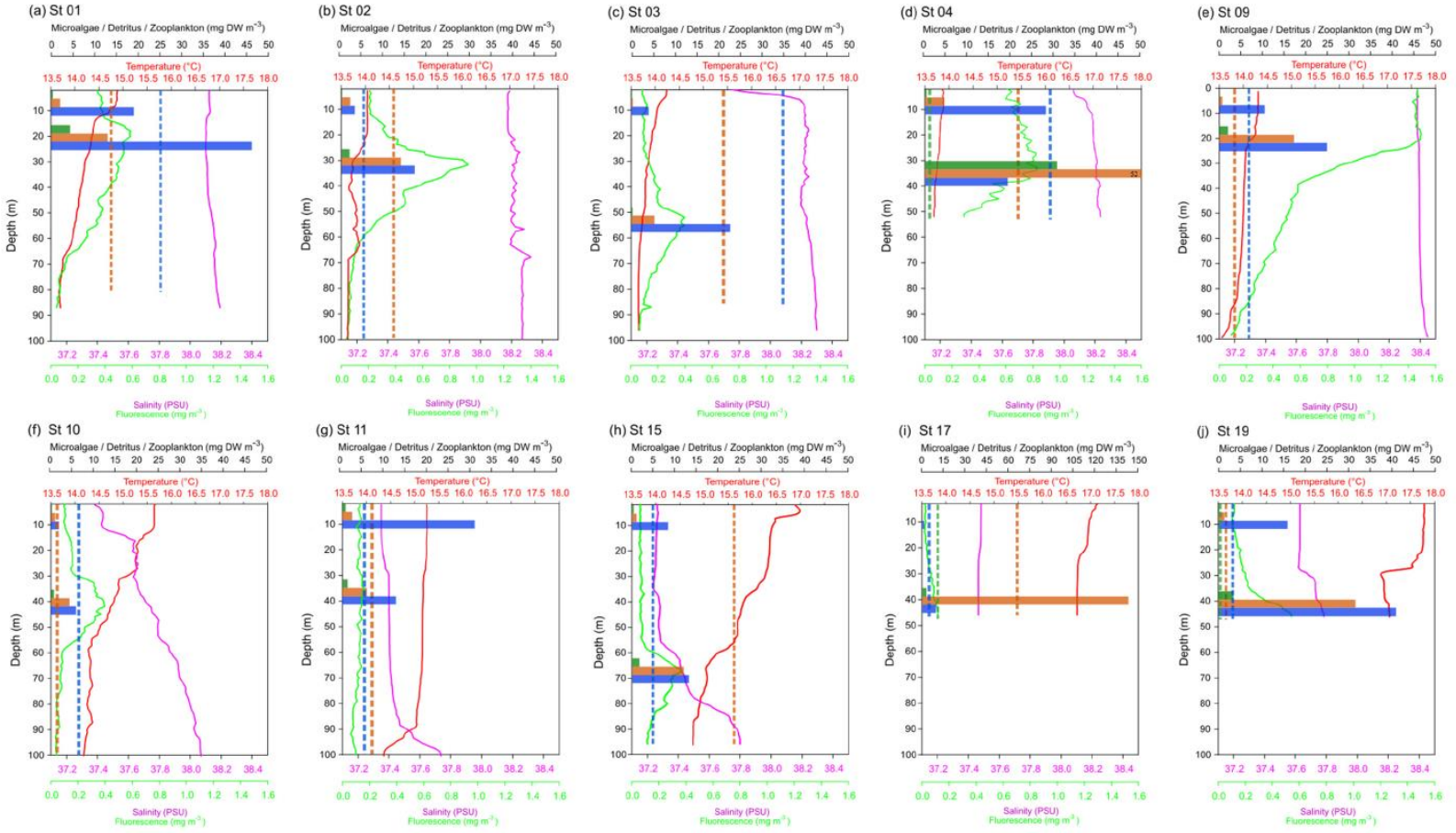

Fig. 4. Vertical profiles of oceanographic variables (temperature, red line; salinity, pink line; and chlorophyll, green line) for all stations (a to j) during the MERITE-HIPPOCAMPE cruise. Biomass of microalgae (green bars), detritus (orange bars) and zooplankton (blue bars) at the surface layer and at CML, and water column-averaged biomass (COL: bottom depth or 200 m deep to the surface) of microalgae (dotted green line), detritus (dotted orange line) and zooplankton (dotted blue line). (For interpretation of the references to color in this figure legend, the reader is referred to the web version of this article.)

sharply decreases down to 0.6 mg Chla m^{-3} at 39 m, and then to 0.1 mg Chla m^{-3} at 98 m. Very high biomass values of microalgae, detritus and zooplankton are recorded in the CML (respectively, 2.2, 16 and 25 mg DW m^{-3}). COL values (200–0 m averaged) for zooplankton and detritus biomass are more than twice as low as at CML. Although detritus and microalgae were negligible in SURF, SURF zooplankton was higher than the COL value. CML is characterized by high dominance of copepods and nauplii, with 78 and 20.3 % respectively, whereas SURF is dominated by copepods with 96 % (Fig. 3a–c).

St10 is situated southwards of the Balearic Front (Fig. 4f). The water column presents different strata with two thermoclines and haloclines respectively around 15 and 30 m, and a CML between 30 and 60 m (0.4 mg Chla m^{-3} at 42 m). Low biomasses of zooplankton, phytoplankton and detritus were found in all strata compared to other stations. COL presents higher zooplankton biomass (6.3 mg DW m^{-3}, on average over the upper 180 m) compared to CML (5.2 mg DW m^{-3}) and surface (2 mg DW m^{-3}). The detritus biomass at CML (4.2 mg DW m^{-3}) is twice as high as at SURF and COL. Microalgae were found only at the CML at a very low value. Zooplankton biomass composition appears different among strata (Fig. 3a–c). CML and COL are quite similar, with copepods dominating the biomass (81 and 74 % respectively). However, COL is differentiated by the contribution of gelatinous organisms and chaetognaths, with respectively 10 and 6 % of the biomass. SURF is characterized by the dominance of copepods, crustaceans, and nauplii (41, 30 and 13 %, respectively).

St11 is situated southwest of Sardinia (Fig. 4g). The water column presents a deep thermocline and a halocline around 88 m, and a homogeneous fluorescence profile with values between 0.1 and 0.2 mg Chla m^{-3}, with the maximum situated at 35 m. Low biomass values of microalgae were collected, with the highest value in the CML (1 mg DW m^{-3}). SURF surprisingly presents high values of zooplankton biomass (30.2 mg DW m^{-3}), more than twice as high as CML (13.8 mg DW m^{-3}) and six times higher than COL (5.8 mg DW m^{-3} averaged value over 182 m). Detritus biomass shows its highest values in COL (7.1 mg DW m^{-3}) compared to CML (5.4 mg DW m^{-3}), and low values at the SURF (2.6 mg DW m^{-3}). The zooplankton biomass presents high dominance of copepods at SURF (91 %) but not at the CML (54 %) due to a high proportion of crustaceans (28.3 %,), whereas in COL chaetognaths and gelatinous organisms were other major contributors (22.3 %) (Fig. 3a–c).

St15 is situated on the shelf of the Gulf of Hammamet on a 100 m depth sea floor (Fig. 4h). The vertical profiles show steps of decreasing temperature values with depth, associated with similar steps of increasing salinity, probably corresponding to different layers. The fluorescence profile shows a peak between 59 and 67 m, thus above the bottom boundary layer. Microalgae were found at the CML. The zooplankton biomass distribution is "classical", with the highest biomass accumulated at the CML (13.1 mg DW m^{-3}), twice the average value of COL (5.25 mg DW m^{-3}, over the 85 m). Detritus biomass was higher in COL than in the CML (24.4 and 13 mg DW m^{-3}, respectively) and even higher compared to SURF (0.97 mg DW m^{-3}). Contributions of zooplankton taxa to biomass presented strong differences between the three strata (Fig. 3a–c). In CML, copepods and crustaceans dominate with 54 and 38 % respectively, whereas only copepods almost dominate SURF strata with 91 %. COL was characterized by the highest percentage of gelatinous organisms and chaetognaths, 54 and 9.2 %, respectively.

St17 is situated in the north of the Gulf of Gabès (Fig. 4i). The water column shows a light thermocline at 23 m and a homogeneous salinity profile. The fluorescence profile presents values of 0.02 mg Chla m^{-3} at the surface and a regular weak increase with depth down to the bottom. Microalgae are found at COL and CML. Comparable zooplankton biomasses are found in CML and COL (9.9 and 10.6 mg DW m^{-3}, respectively) whereas biomass is very weak in SURF. Very high detritus biomass cumulates in the CML (138.6 mg DW m^{-3}) in contrast with the lack of detritus in SURF (0.35 mg DW m^{-3}), whereas COL presented an intermediate value. The contribution of zooplankton taxa to biomass in the 3 strata slightly changed (Fig. 3a–c), although copepods dominate in all three. Gelatinous organisms and chaetognaths are recorded with 6 and 5 % for the COL but disappeared in SURF. The CML was characterized by a high presence of nauplii with 26 % and miscellaneous at 11 %.

St19 is the southern station in the Gulf of Gabès in shallow water (Fig. 4j). A thermocline and a halocline occur around 30 m. The fluorescence profile presents values of 0.11 mg Chla m^{-3} at the surface, and regularly increases down to the bottom 0.54 mg Chla m^{-3}. Microalgae were found at the CML. The detritus biomass at the CML (31.4 mg DW m^{-3}) is much higher than in COL (2 mg DW m^{-3}) and SURF. CML zooplankton biomass (41.6 mg DW m^{-3}) was double the biomass measured in SURF (16 mg DW m^{-3}) and was much higher than in COL. Copepods dominated zooplankton in all strata (Fig. 3a–c), whereas SURF differed by more crustaceans, CML by more miscellaneous, and COL by more gelatinous organisms.

3.4. Zooplankton and detritus biomass in different size-fractions in the CML

Fig. 5a shows the details of the distribution between sieved-size fractions of the biomass (see Section 3.2 and Table 2) collected with the Hydro-Bios net in the CML (Fig. 3e). In general, detritus were concentrated in the lowest size fractions, and absent above 1000 µm, and similarly, the Hydro-Bios net-retained microalgae accumulated in the smaller fractions, mostly in fraction 60–200 µm, plus in fraction 200–500 µm for St04 and 17. In contrast, zooplankton was distributed in all fractions with no clear pattern of dominance in a given size fraction among the stations. When detritus and microalgae biomasses were high in the first smaller fractions, zooplankton biomass was generally low in the largest fractions.

The percentages of zooplankton taxa biomasses (Fig. 5b) were dominated by copepods and nauplii in the first smaller fractions, except at stations St17 and St19 where other plankton (miscellaneous) contributed substantially. At all stations, except St04, the fraction 200–500 µm was strongly dominated by copepods (>71 %). At many stations, copepods still dominated the fraction 500–1000 µm (St01, 02, 03, 04, 09, 10, 19 > 80 %) and even the fraction 1000–2000 µm (St01, 02, 09, 10, 11). In the three largest fractions, crustaceans other than copepods could heavily dominate the biomass at some stations (St01, 02, 03, 09, 15 > 52 %), whereas at other stations, gelatinous organisms (St03, 10, 11, 19) and chaetognaths (St10, 11, 15) could make noticeable contributions. Appendicularians occur at some stations (St01, 04, 09) in the three smaller fractions, but with negligible biomass.

3.5. Comparisons of collected zooplankton and detritus biomasses in size fractions between CML and COL

In all stations, the contribution of the fraction 60–200 µm (Fig. 6a) to the total zooplankton biomass in COL-60 was weak, i.e., <9 %, except <17 % for St02, the biomass being distributed mostly in the fractions 200–500 µm and >500 µm but rather unequally and without a regular pattern between stations. The distribution patterns of zooplankton among size classes were not always entirely similar between COL-60 and CML (Figs. 6a and 5a), with the interesting exception of stations St03 and St15 where biomass concentrations increase with size-classes. It is noticeable that the contribution of the small fraction to the zooplankton biomass in CML was on average 2.5 times higher than in COL, and significantly different (Table 3).

In contrast to zooplankton distributions, detritus biomass in COL-60 (Fig. 6a) is concentrated in the two first size-classes, mainly the first one (60–200 µm), and a very low contribution for the fraction >500 µm (see average values on Table 3). This pattern is different from that of CML (Fig. 5a), where the contribution of the smaller fraction to biomasses was on average twice as low as in COL-60 (Table 2), whereas this contribution was much higher in the fractions above 200 µm. This shift

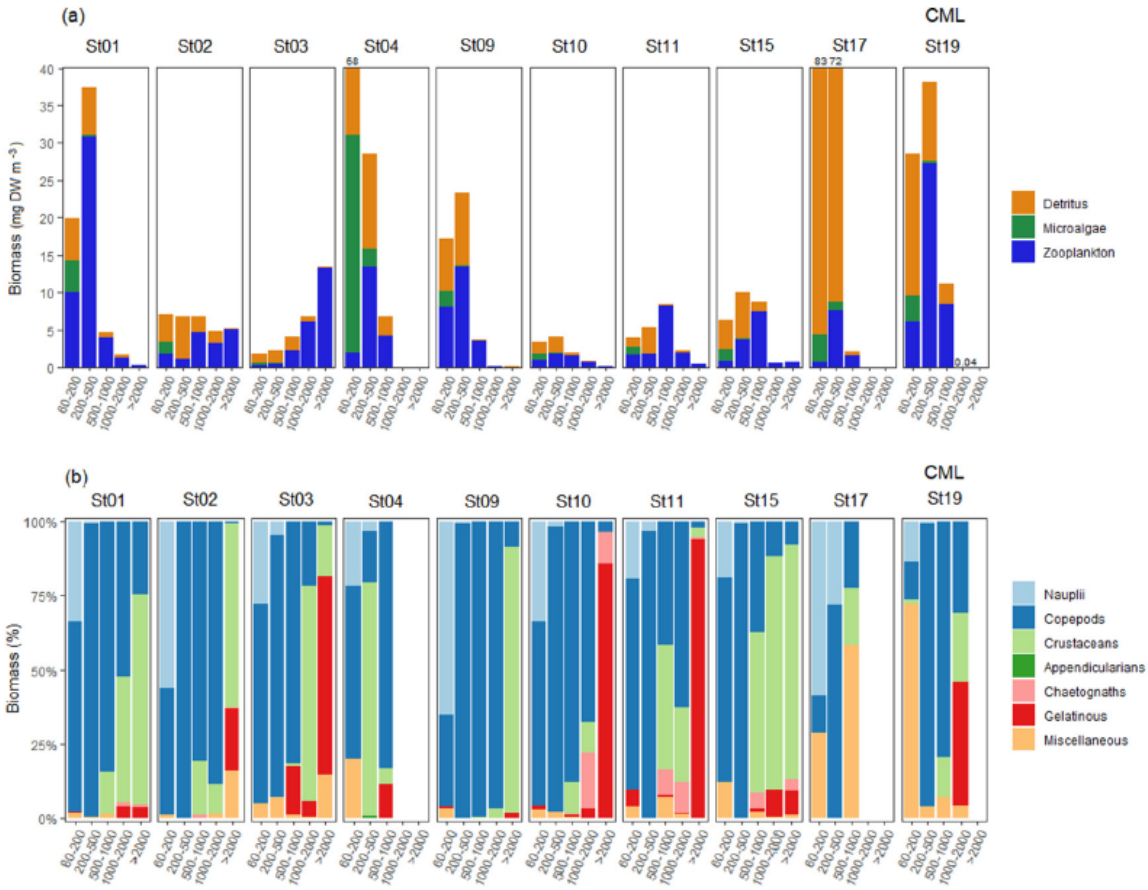

Fig. 5. Plankton and detritus biomasses collected with the Hydro-Bios tow using 60 µm mesh-size net at Chlorophyll Maximum layer (CML) at the different stations during the MERITE-HIPPOCAMPE cruise. (a) Cumulated biomass concentrations (mg DW m^{-3}) of zooplankton (blue), microalgae (green), and detritus (orange), and (b) cumulated percentages of zooplankton taxa biomasses, in the five size fractions. Note that: (1) fraction 1000–2000 µm is missing for stations St04 and St17, and the fraction >2000 µm is missing for stations St04, St17, and St19; (2) In the top panel for St04, 17, and 19 the numbers on the top of the bars the value reached by the cumulated biomass. (For interpretation of the references to color in this figure legend, the reader is referred to the web version of this article.)

in contributions of the detrital material in the successive size fractions was confirmed by significant differences between mean values (Table 3). In COL-60, when microalgae are collected, they are mostly present in the first class (Fig. 6a), a characteristic common with sampling in the CML.

In terms of taxonomic contributors to zooplankton biomass of COL-60 (Fig. 6b), nauplii and miscellaneous counterbalance, and sometimes dominate small copepods in the smaller fraction (60–200 µm). The fraction 200–500 µm is most often strongly dominated by copepods and completed by gelatinous organisms, excepted at St15 where gelatinous organisms dominate. Large copepods generally dominate the biomass in larger fractions (>500 µm), but some stations present high contributions of gelatinous organisms and crustaceans (St03, 10, 11, 15, and 17). The contribution of crustaceans is high in CML both for the total biomass and for the fractions above 500 µm. Inversely, the contribution of gelatinous organisms (and chaetognaths at a few stations) is much higher in COL-60 than in CML. These trends are confirmed by significant differences between mean values (Table 3).

3.6. Estimated zooplankton carbon demand and nitrogenous and phosphorous excretion

The daily carbon demand of zooplankton ranged from 0.6 to 6.9 mg C m^{-3} d^{-1} at the CML and from 0.5 to 5 mg C m^{-3} d^{-1} in COL, with the highest values at St19 for both strata (Fig. 7a–d). The mean values show no significant difference between the two strata (paired *t*-test; $p = 0.21$). When excluding the contribution of carnivorous forms (chaetognaths), this ZCD represented 2.7 to 22.7 % of the phytoplankton stock per day at the CML and between 3.1 and 25 % in COL, with no significant difference between the mean values of the two strata (paired *t*-test; $p = 0.29$). This grazing pressure showed no clear spatial trend at the CML, but in COL the values were on average significantly lower at the northern stations (St01 to St09; mean = 7.3 ± 3.3 %) than at the southern stations (St10 to St19; mean = 19.6 ± 6.0 %), in association with a parallel and significant decrease of the phytoplankton biomass from 27.4 ± 20.2 mg C m^{-3} in the north to 7.8 ± 6.1 mg C m^{-3} in the south (Mann-Whitney *U* tests; $p = 0.036$ and 0.0002, respectively).

The daily nitrogen and phosphorous excretion (Fig. 7b–e and c–f, respectively) varied between 4 and 908 µg N m^{-3} and between 0.5 and 131 µg P m^{-3}, respectively, and were not significantly different between the DCM and COL (paired *t*-test; $p > 0.3$). The zooplankton excretion represented a daily N and P recycling equivalent to 0.2 to 19 % of the DIN stock and to 0 to 21 % of the DIP stock. In both cases the highest values were found at the DCM of St01 in relation to the very high zooplankton biomass at this level (see Fig. 4a).

The contribution of the different size fractions to the ZCD was highly variable between stations and strata (Fig. 8). The contribution of the smaller fraction (<500 µm) to the ZCD is more often highly predominant or at least comparable to that of larger fractions (>500 µm), except at St19 for COL and at St03 in CML where most of the ZCD (>80 %) was from the larger fraction (>500 µm). On average, the relative contribution of the size-fractions to the ZCD showed no significant difference between CML and COL (paired *t*-test; $p > 0.1$).

Considering the whole size-fractions, copepods were the major contributors to the ZCD, except in the CML at St04 where other crustaceans made an equivalent contribution (46.9 % vs 47.3 % for copepods). Other crustaceans also made an important contribution to ZCD

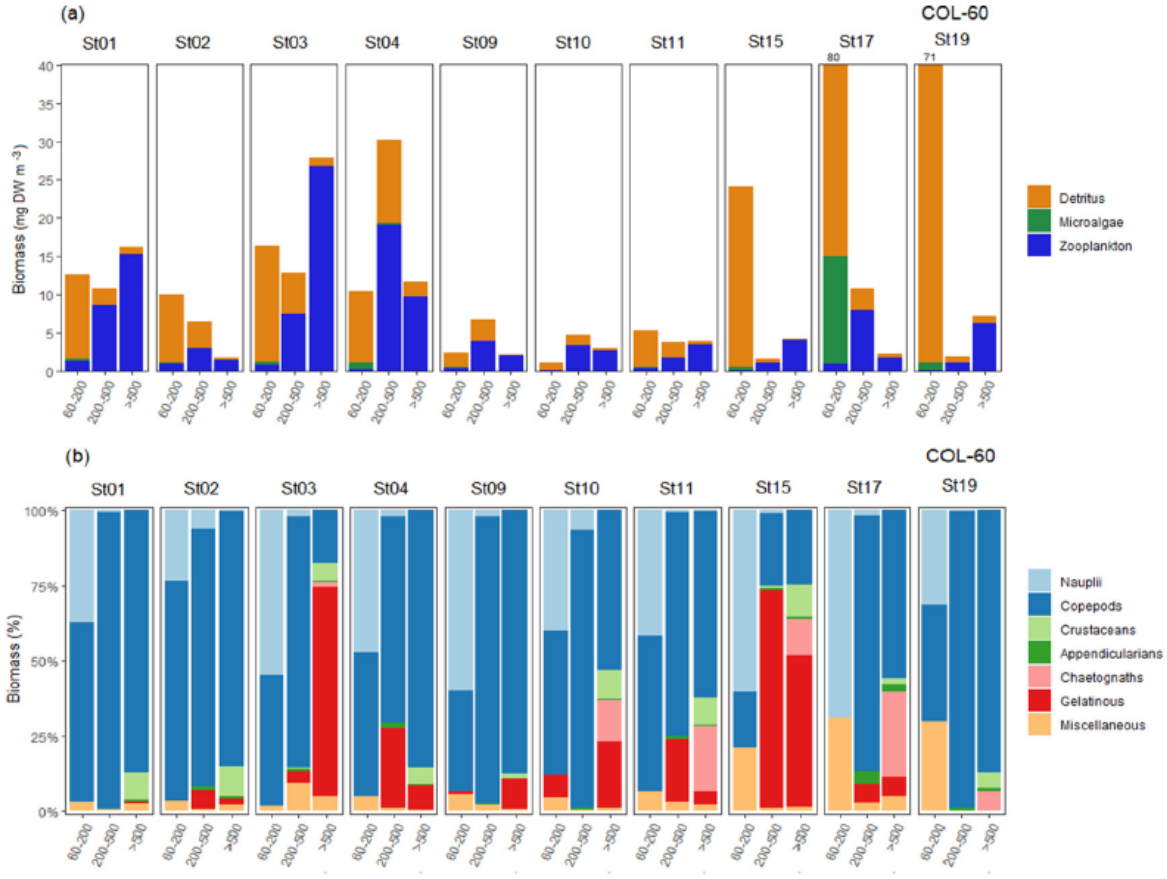

Fig. 6. Plankton and detritus biomasses collected with the vertical net tow using 60 µm mesh-size net (COL-60) at the different stations during the MERITE-HIPPOCAMPE cruise: (a) Cumulated biomass concentrations (mg DW m^{-3}) of zooplankton (blue), microalgae (green) and detritus (orange), and (b) cumulated percentages of zooplankton taxa biomasses, in the three size fractions. Note that: In the top panel for St17 and 19 the numbers on the top of the bars were the value reached by the cumulated biomass. (For interpretation of the references to color in this figure legend, the reader is referred to the web version of this article.)

in the CML at St15 (34.5 %) and St02 (25.4 %), whereas miscellaneous zooplankton was numerous in the CML at St19 (21.9 %) and gelatinous organisms in the COL at St03 (18.4 %) and St15 (28.5 %). On average, copepods contributed significantly more to the ZCD in COL than in CML, and the same trend was observed for gelatinous organisms and appendicularians, whereas nauplii contributed more to the ZCD in CML than in COL (paired *t*-test; $p < 0.05$). Overall, the total ZCD, and the contribution of size fractions or of taxa to this ZCD showed no clear spatial pattern.

The contributions of size-fractions or the taxa to N and P excretion rates were very similar to those of ZCD (i.e. similar to Fig. 8). All values for ZCD and excretion rates are presented in the supplementary material.

4. Discussion

4.1. Overview of the spatial patterns of environmental and biological variables during the MERITE-HIPPOCAMPE cruise

As the campaign took place over one month in the spring along a north-south transect with 10 stations sampled, either on the way out or on the way back, the environmental and biological characteristics of the stations did not enable a clear regional spatial pattern to be obtained, and local climatic and hydrodynamic conditions predominated over the spatial gradients. This means that the results obtained on the biotic compartment and ultimately in the contaminant studies must be interpreted in a mostly local context. Nevertheless, the present work contributes to broadening the characterization of plankton and detritus biomass distribution in the three different strata over several regions in the Mediterranean Sea.

We could highlight some global differences between the stations located north and south of the Balearic front, in terms of temperature and salinity values (see Fig. 2), in phytoplankton biomass in both COL and CML (see Fig. 7a and d), but only for COL in zooplankton grazing (see Fig. 7a). These patterns are probably linked to a late impact of the deep winter convection in the Gulf of Lion in 2019, a relatively convective and productive year (Margirier et al., 2020; Bosse et al., 2022), in the northern part of our transect (i.e. down to the Balearic front), whereas the generally low plankton productivity of the southern region can be increased by long-term mesoscale features isolated from the Atlantic current (Millot and Taupier-Letage, 2005), such as at our stations 10 and 11 (Rwawi et al., 2023), or by the impact of Saharan dust (Riandey et al., 2005; Feliú et al., 2020; Guieu et al., 2020) such as at our stations 10, 11 and 19 (Tedetti et al., 2023).

Some differences between coastal (St01, 03, 04, 15, 17, and 19) and open sea stations (St02, 09, 10, and 11) in terms of detritus and zooplankton biomasses (see Fig. 3g) could be linked in coastal stations to resuspension of sedimentary particulate matter induced by local wind-driven currents, and for zooplankton to limited deep vertical migration compared to open sea stations (since sampling was always performed during daylight, when most zooplankton are found in deeper water). However, the zooplankton biomass (total and in taxonomic contribution) does not show any specific gradient from north to south whatever the strata or the net considered (see Figs. 1b and 3). It is likely that the small number of sampled stations, especially in oceanic areas, as well as the long duration of our campaign do not allow identification of large north-south patterns that have nevertheless been widely documented for zooplankton in other studies (Mazzocchi et al., 2007; Siokou-Frangou et al., 2010; Nowaczyk et al., 2011; Saiz et al., 2014). Moreover, these studies have also mentioned that more local hydrodynamic or atmospheric conditions occur in addition to these large global patterns.

Table 3
Summary of the biomass for plankton and detritus, and size fractions during the MERITE-HIPPOCAMPE cruise. Mean and SD estimated of total biomasses for detritus, microalgae and zooplankton and percentage for size fractions and zooplankton taxa at CML and COL. Comparison between mean values based on paired *t*-test on non-transformed and log-transformed data (with respectively symbols * and ** for significant differences), and (1) significant but without reaching necessary conditions.

	CML		COL		*t*-Test on difference
	Mean	SD	Mean	SD	
Detritus (mg DW m^{-3})	29.08	42.26	20.23	20.52	
% 60–200	39.98	16.42	69.52	23.17	*, **
% 200–500	47.07	13.08	26.29	21.10	*
% >500 (n=7)	16.47	14.46	4.18	3.37	**
Microalgae (mg DW m^{-3})	5.26	9.36	5.81	16.95	
% 60–200	90.29	5.12	90.51	11.62	
% 200–500	9.71	5.12	9.49	11.62	
% >500 (n=7)	–	–	–	–	
Zooplankton (mg DW m^{-3})	20.40	13.33	13.69	11.46	
% 60–200	13.53	8.48	5.78	4.99	*, **
% 200–500	42.77	27.12	43.00	21.33	
% >500 (n=7)	54.22	31.58	51.22	23.50	
Total biomass in percentage					
Nauplii	8.07	8.54	3.57	2.54	(1)
Copepods	62.19	22.46	69.22	23.13	
Crustaceans	17.98	18.80	3.57	2.54	**
Chaetognaths	1.35	2.19	4.01	4.65	**
Appendicularians	0.06	0.17	0.97	1.01	(1)
Gelatinous	5.49	13.09	16.04	20.79	**
Miscellaneous	4.86	4.88	2.62	1.76	
Biomass fraction 60-200 in percentage					
Nauplii	34.84	18.57	46.33	14.42	
Copepods	48.94	22.87	41.57	20.67	
Crustaceans	0.14	0.44	0.01	0.03	
Chaetognaths	–	–	–	–	
Appendicularians	0.01	0.05	–	–	
Gelatinous	0.74	1.68	0.86	2.39	
Miscellaneous	15.33	22.03	11.23	11.44	
Biomass fraction 200–500 in percentage					
Nauplii	4.37	8.50	2.22	2.25	
Copepods	86.26	25.66	80.64	22.14	
Crustaceans	7.86	24.86	0.09	0.18	
Chaetognaths	–	–	–	–	
Appendicularians	0.08	0.25	1.16	1.19	(1)
Gelatinous	0.00	0.00	13.62	22.66	
Miscellaneous	1.43	2.44	2.26	2.74	
Biomass fraction >500 in percentage (n=7)					
Nauplii	0.02	0.04	0.03	0.04	
Copepods	59.19	28.82	64.51	26.69	
Crustaceans	26.26	18.14	6.87	3.35	**
Chaetognaths	3.08	3.53	8.40	10.27	
Appendicularians	0.01	0.01	0.66	0.67	(1)
Gelatinous	8.51	15.79	17.40	23.83	
Miscellaneous	2.94	3.41	2.13	1.73	

Bold characters indicate higher significant mean values.

For each station, our study strategy enabled us to identify vertical gradients provided that recent local climatic and hydrodynamic conditions did not lead to excessive mixing (see Fig. 4). Some stations (St01, 02, 03, 10, and 15) showed a rather typical stratification with clear vertical physical gradients and a maximum of chlorophyll, but this was not systematically reflected in the zooplankton biomasses. For various reasons, other stations did not show clear stratification. Station 04 had among the highest zooplankton biomass at the surface, probably related to a homogenization of the water column. Very shallow coastal stations in Tunisia showed accumulations of Chl*a* and zooplankton in a CML just above the bottom (St17 and St19). This phytoplankton biomass bulk above the bottom where zooplankton accumulates as well is a phenomenon also encountered in the Gulf of Lion (Espinasse et al., 2014). These Tunisian coastal stations (St15, 17, and 19) did not show high zooplankton concentrations in the water column compared to the northern coastal stations (St01, 03, and 04). This may be more related to their high detritus load than to differences in community structure when compared to the northern coastal stations. This detritus load may be a consequence of mixing and retention due to the high tidal currents in the Gulf of Gabès (Béjaoui et al., 2019).

The oceanic offshore stations presented a quite different pattern for the reasons explained below. Station 09 is located in the usual area of the deep-convection (Margirier et al., 2020). Although it was visited at the end of the survey (8–9 May), which was a little more than one month after the peak of the phytoplankton bloom observed at the end of March, it was the richest station in Chla, nitrate and silicate from the whole MERITE-HIPPOCAMPE cruise (Tedetti et al., 2023). Station 09 had a true mixed layer above the CML up to the surface, inducing higher Chla and zooplankton concentrations in CML and SURF, compared to COL (see Fig. 4e). Although the stratification appeared quite moderate (almost homogeneous temperature and salinity), the high chlorophyll in the layer 0–25 m might be due to previous steps of stratification and to mesoscale structures in this area in this period (Rwawi et al., 2023). Similar high zooplankton concentrations present in the upper layer in the post-bloom phase in the deep-convection area have already been described by Donoso et al. (2017). Station 02 is an oceanic station, situated in the broad periphery of the deep convection area (following Donoso et al., 2017), very close to the coast but also impacted by other different phenomena: intrusions of the northern current, hydrodynamic processes linked to the shelf break, and coastal impacts. This station sampled in the early phase of the cruise, under very bad weather conditions, presented a clear CML, despite a homogeneous physical structure. It is separated from the open ocean by the North Current and is not much affected by deep convection due to this natural barrier (Millot and Taupier-Letage, 2005). Zooplankton sampling at stations 10 and 11 in the western oceanic waters of Sardinia was performed with a time lag of one day and occurred respectively 2 and 3 days after a dust event (22 April). The zooplankton biomass and taxonomic structure showed an interesting contrast between these two stations, particularly with differences in surface (Figs. 3b and f; 4f and g), which could be consistent with zooplankton quick response to dust effect in a few days (Feliú et al., 2020). In contrast, differences in CML (Fig. 3a and e; Fig. 4f and g), not comparable to those observed at the surface, might be rather due to an additional specific 3D-mesoscale context of each station (Rwawi et al., 2023) impacting the vertical structure and differentiating the SURF and CML layers (see Fig. 4f and g), and the integrated values over the water column appeared buffered (Figs. 3c and g; 4f and g). For the oceanic station 11, the water column seems very homogeneous down to 90 m, with a very low Chla maximum, and the low zooplankton biomass from the vertical net in the upper 200 m is due to the very low biomass below 90 m. The very high value for zooplankton at the surface may be due to enhanced productivity since a high density of copepodites stages was observed (Makhlouf, pers. comm.).

4.2. *Biological specificities of the CML*

Due to the sampling strategy centered on the CML layer for measurements of contaminant contents in plankton, our focus on zooplankton characterization in the CML appears to be unique compared to previous regional studies in the Mediterranean Sea. Zooplankton net sampling is usually carried out by vertical net tows in the epipelagic zone (0–200 m) or just under the surface layer when studying the hyponeuston. These two types of sampling were also carried out during the MERITE-HIPPOCAMPE cruise to allow better characterization of the CML by comparisons with other strata.

At the scale of the basin, this comparison shows first of all an accumulation of detritus most often occurring at the CML, whereas SURF always presented the lowest detritus loads (see Fig. 4). Sometimes the CML was also a layer of accumulated microphytoplankton, mostly chain-aggregated and/or linked to detritus e.g. station 04 (see Fig. 4d). Among

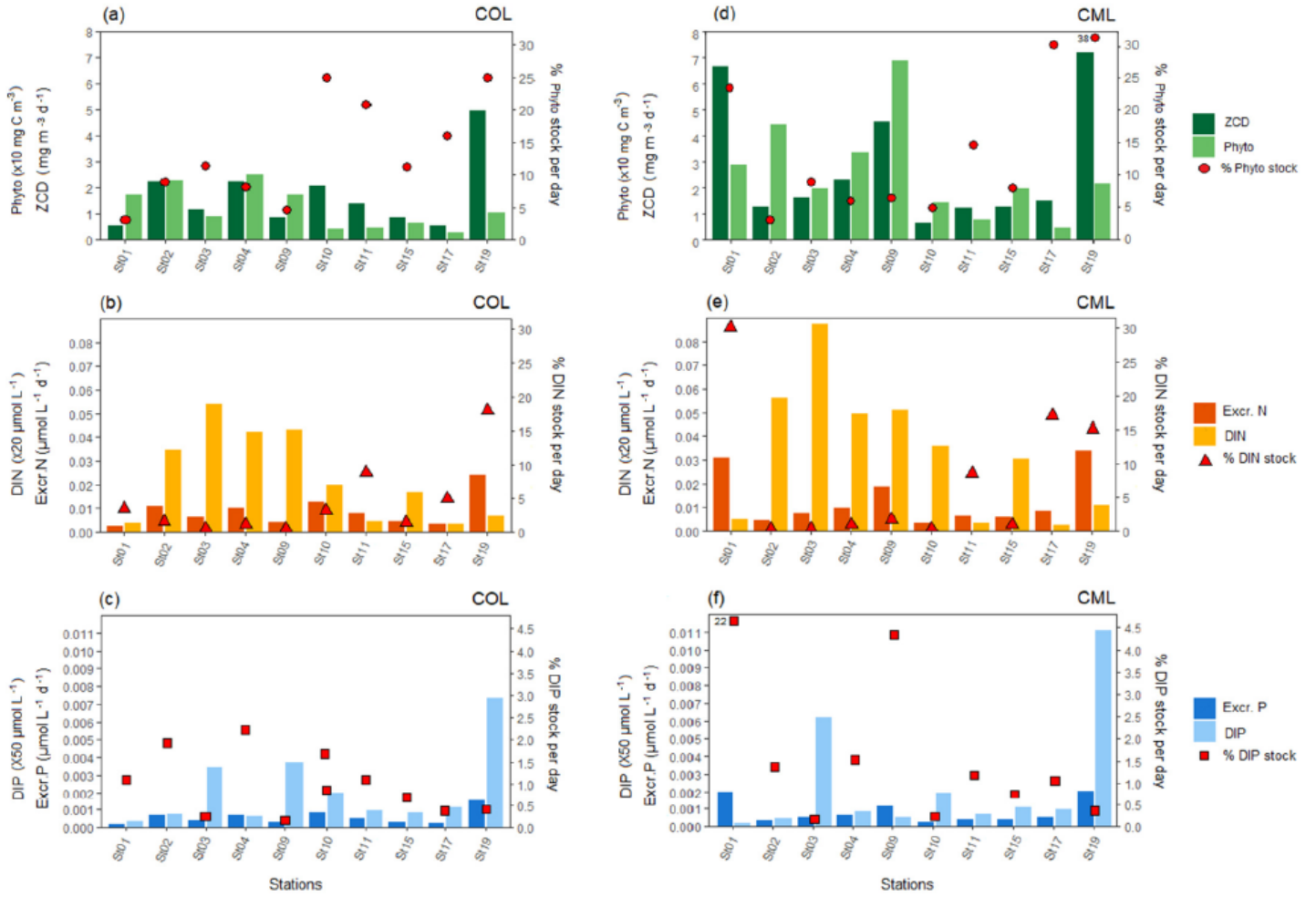

Fig. 7. Zooplankton carbon demand and phytoplankton stock, and percentage on the ratio (a, d), nitrogen excretion and DIN stock, and percentage on the ratio (b, e), phosphorous and DIP stock, and percentage on the ratio (c, f), respectively for COL (a, b, c) and CML (d, e, f). Note: In panel (f) the number for station 01 gives the value of %DIP stock out of scale.

all stations, zooplankton biomass was on average higher at the CML than in COL and SURF (respectively 1.5 and 1.7 times higher), but the differences between the 3 strata were not statistically significant due to very high variability. According to the stratification and the intensity of the chlorophyll peak around the identified CML in each station profile, we can indeed distinguish 4 cases: (1) no accumulation of zooplankton at the CML when the peak is not well-formed (St04, 11, and 17), (2) accumulation of zooplankton at the CML when the peak is well-formed (St01, 02, 15, and 19) but also (3) no accumulation despite a well-formed peak (St03 and 10), and finally (4) the case of station 09 is a bit different with a high concentration of zooplankton at the CML but with a 0–25 m layer quasi-uniformly rich in Chl*a*.

Our observations were not dedicated to the fine characterization of vertical profiles of phytoplankton, marine snow, and zooplanktonic groups, as shown in recent studies such as those described by several authors (e.g. Möller et al., 2012; Lombard et al., 2019; Briseño-Avena et al., 2020) using combinations of video sensors and net hauls enabling correlation of the aggregation layers to detrital and planktonic particles. However, our observations can be analyzed in the light of patterns described in these articles. Accumulation of detritus (marine snow) and large phytoplankton the most often slightly below the CML has been already documented in many situations. Very often, accumulation of zooplankton occurred as well (Nowaczyk et al., 2011; Möller et al., 2012; Espinasse et al., 2014; Saiz et al., 2014; Fender et al., 2019; Briseño-Avena et al., 2020), but was quite variable between taxa as shown by video observations (Möller et al., 2012; Briseño-Avena et al., 2020). In particular the aggregation of nauplii, copepodites and small copepods at the CML was already described during the stratification period in the Mediterranean (Alcaraz, 1985, 1988; Alcaraz et al., 2007; Sabatés et al., 2007, 2008; Olivar et al., 2010; Nowaczyk et al., 2011; Saiz et al., 2014), showing that this chlorophyll-rich layer constitutes a favorable habitat for the reproduction of copepods, particularly in oligotrophic conditions, where the CML can be considered as an "oasis" to sustain secondary production (Saiz et al., 2014). The high biomass of crustaceans recorded in the CML (mainly euphausiids larvae) may be explained by an adaptation of their vertical migration to track the most favorable trophic conditions, as reported in several studies (Sameoto, 1986; Guglielmo et al., 2011; Granata et al., 2020).

Inversely, gelatinous filter feeders (appendicularians, salps and doliolids) seem to avoid the CML, in agreement with many previous observations (Fenaux, 1968; Paffenhöfer et al., 1991; Briseño-Avena et al., 2020). In this layer, these filter-feeders might be disturbed by high accumulation of detritus and large algal cells leading to a decline in food quality (López-Urrutia et al., 2003) and/or to house clogging in the case of appendicularians (Tiselius et al., 2003; Feliú et al., 2020). The low abundance of chaetognaths and (presumably) of other gelatinous carnivorous organisms at the CML is rather surprising because we might have expected to high concentrations of these carnivorous organisms at a level where the stock of zooplankton prey would be more abundant. This could be related to day-night migration strategies, where these groups would be present in deeper waters during the day, thus avoiding larger predators (Granata et al., 2020). Their scarcity in our Hydro-Bios samples could be also linked to their active swimming out of the capture path of the net probably favored by a quicker net clogging compared to

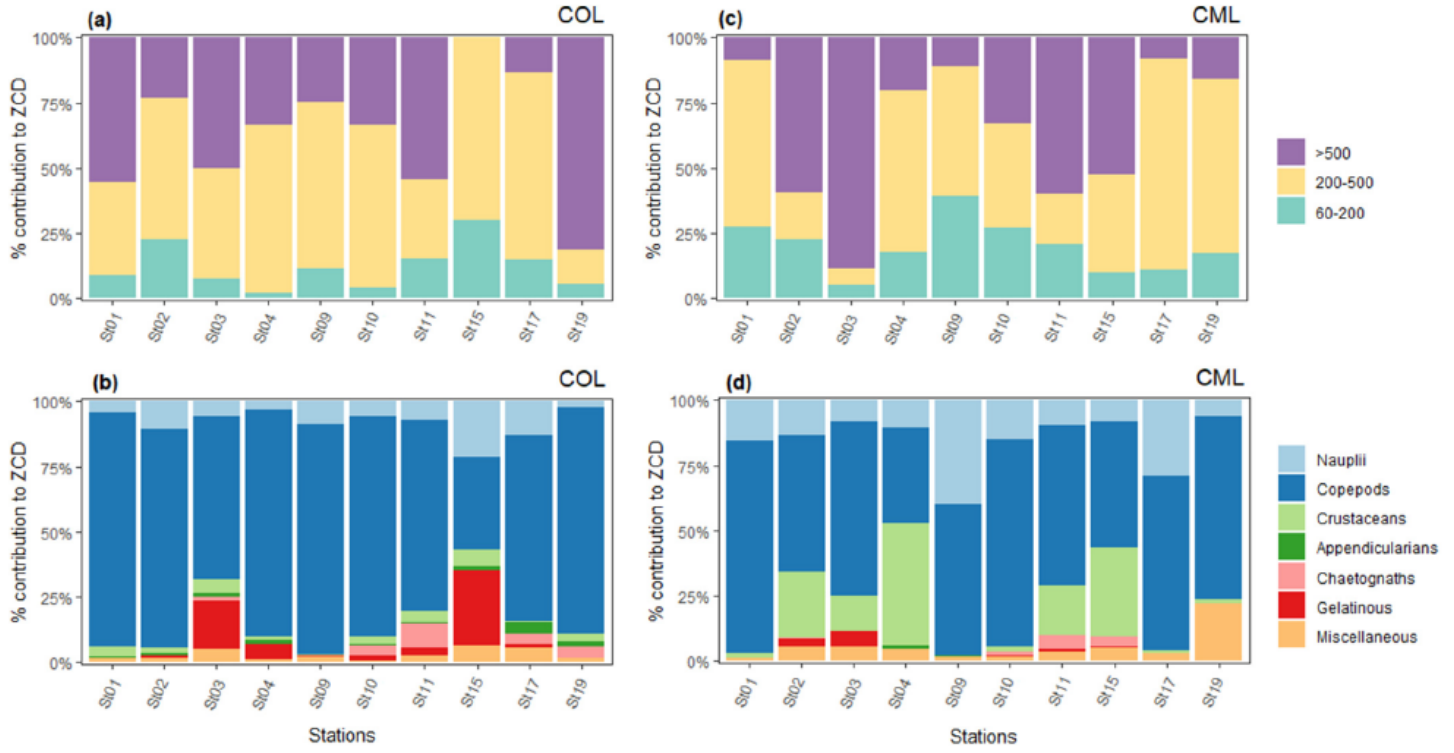

Fig. 8. Contributions in cumulated percentages of size-fractions (a, c) and zooplankton taxa (b, d) to the zooplankton carbon demand in COL (a, b) and CML (c, d).

the vertical net (Sameoto et al., 2000).

Such aggregation of matter and plankton linked to the CML has relevant implications for the functioning and structuring of the pelagic food web in the Mediterranean (Saiz et al., 2014). In our study, the high biomass of zooplankton over a wide size spectrum (from nauplii to large crustaceans) and its intense metabolic activity shown by high ZCD and excretion values are signs of increased trophic fluxes at this level. High densities of larvae of small pelagic zooplanktivorous fish such as anchovy have been reported as well (Sabatés et al., 2007, 2008; Olivar et al., 2010), showing the importance of CML for the trophic transfer of matter and contaminants towards higher trophic levels.

4.3. *Characterizing the biota in size fractions to interpret biogeochemical and contaminant fluxes*

The first characteristic of our Hydro-Bios samples is the high proportion of detritus, mainly in the size-fractions below 500 µm at all stations. Thus, the interpretation of contaminant levels in these fractions must be done cautiously to take account of a potential bias linked to these detritus content which may have various (mineral or organic) origins. In this paper, we have not gone into a detailed description of the nature of the detritus particles. These detritus probably have different sources and compositions in the coastal zone (resuspension of inorganic and organic particles from the sediment in addition to pelagic production of detritus particles) and the offshore zone (pelagic detritus particles to which may be added particles from atmospheric inputs). As mentioned in Section 4.2, patterns of vertical distributions of detrital particles which accumulate below the productive layer in the water column have already been well documented. This may have consequences for the biogeochemical cycles of contaminants and their accumulation/transfer processes in planktonic food webs in the Mediterranean Sea. Firstly, suspended particles (microphytoplankton and detrital particles) represent active surfaces for the adsorption and absorption of hydrophobic contaminants (Castro-Jiménez et al., 2021). Secondly, these suspended particles are also the site of intense microbial activity (Dolan and Marrasé, 1995; Azam and Long, 2001) which can certainly play a role in the accumulation and transfer of contaminants (da Fonseca et al., 2022; Chifflet et al., 2023), some components of which, such as ciliates, are known to be the preferred prey of mesozooplankton (Saiz and Calbet, 2011). And thirdly, a large part of these particles will sink (depending of their size and shape) and will export matter and contaminants into deeper layers (Bouloubassi et al., 2006; Bacosa et al., 2020) potentially integrated in the mesopelagic food-web (Romero et al., 2018). In the case of our MERITE-HIPPOCAMPE cruise, the fractions below 500 µm were much more impacted by detritus and microalgae at St04 and St17 (>90 %) than at St01 and St09 (~50 %), which clearly induced differences in biochemical compositions (see Fig. 3 in Tesán-Onrubia et al., 2023 and Fig. 3 in Guigue et al., 2023) and contaminant levels (see Fig. 5a,c in Guigue et al., 2023; see Table S4 in Chifflet et al., 2023).

The second characteristic concerns the trophic types of the dominant zooplanktonic species within the two smallest fractions (60–200 and 200–500 µm) which modulate the associated impacts on estimate fluxes. In MERITE-HIPPOCAMPE, when these fractions presented zooplankton biomass dominated by herbivorous and omnivorous types (small copepods and nauplii, or small pteropods), they showed isotope ratios $\delta^{13}C/\delta^{15}N$ confirming a trophic level around 2 (Tesán-Onrubia et al., 2023), relatively higher trophic fluxes (our Figs. 5 and 7) and contaminant contents (see Fig. 5c in Guigue et al., 2023; see Fig. 2 and Table S4 in Chifflet et al., 2023), such as for stations St01, 04, 09, and 19. This key role of herbivorous zooplankton in contaminant transfer has been already demonstrated in high latitude ecosystems where a few species massively dominate (e.g. Foster et al., 2012).

The third characteristic concerns the large fractions. First, the sampling of these fractions in our study was certainly impacted by clogging with detritus and microphytoplankton, favoring net avoidance of large organisms, and inversely explains their higher proportion for stations with low biomasses of detritus and microphytoplankton (e.g. St03). Moreover, it is also crucial to define the dominant trophic types in planktonic fractions >500 µm. During MERITE-HIPPOCAMPE, these fractions were either marked by the presence of typical carnivores, mainly chaetognaths, hydromedusae and siphonophores (St03, 10, 11, see Fig. 5b), or the presence of large crustaceans dominated by euphausiids and decapods (St01, 02, 09 and 15). Increased proportions of

carnivorous zooplankton in largest size fractions compared to smallest fractions (<500 µm) strongly dominated by herbivorous/omnivorous organisms, were already reported in the Gulf of Lion (Espinasse et al., 2014) and in the Bay of Marseille (Tiano et al., 2014). It is noticeable that ZCD and excretion rates calculated for St03, 10 and 11 were the lowest, linked to the lower weight specific-rates of the larger organisms. This increased proportion of carnivorous forms in the two largest fractions agree with the trophic level (TL) derived from isotopic analyses on the same fractions (Tesán-Onrubia et al., 2023): mean TL around 2.5, with highest values also found at St10 and 11 (TL of 3.6 and 2.8, respectively), suggesting a high proportion of secondary consumers.

Taxonomic determination by very large groups would merit being further refined, especially for copepods whose trophic characteristics vary from pure herbivory to carnivory (Kouwenberg, 1994; Espinasse et al., 2014), and gelatinous plankton, which covers very different trophic groups, from large herbivorous filter feeders (salps, doliolids) to carnivores (jellyfish, siphonophores, ctenophores).

5. Conclusion

The choice of sampling in the CML for this study regarding the role of plankton as a contaminant pump was guided by the aims of (1) collecting a high biomass of plankton from the same location to measure levels of a wide range of contaminants, and over a broad spectrum of planktonic size fractions, and (2) being located in an important area for pelagic trophic interactions in both the coastal and marine areas. The present paper has characterized the nature of the particles and zooplankton collected by the nets at depth and demonstrated the similarities and differences of this planktonic community to that of the water column.

The different distribution patterns of planktonic biomass encountered among the different stations during the MERITE-HIPPOCAMPE campaign should make it possible to compare contrasted situations of the accumulation or not of contaminants in the planktonic food web according to the pattern of these distributions.

By looking at the different size fractions of zooplankton that reflect different trophic levels (Tesán-Onrubia et al., 2023), we have shed new light on the processes of accumulation (or not) of contaminants, particularly in relation to studies where the zooplankton is either taken as a whole (Battuello et al., 2016, with the whole of the zooplankton caught by a mesh size net of 300 µm) or based on particular taxa but requiring their selective collection (Ndah et al., 2022). The method described in this paper, which characterizes successive fine size classes, provides an additional dimension for understanding the functioning of planktonic food webs in contaminant accumulation processes.

Data availability

All data from the MERITE-HIPPOCAMPE cruise (doi:10.17600/18000900; Tedetti and Tronczynski, 2019) is stored in the MISTRALS-SEDOO database (https://mistrals.sedoo.fr/MERITE/) and will be made publicly accessible once all the articles related to the cruise are published in the present special issue. In the meantime, data can be obtained upon request from the corresponding author. In addition, navigation data and CTD profiles from the MERITE-HIPPOCAMPE cruise are available via the IFREMER/SISMER database (https://data.ifremer.fr/SISMER).

Acknowledgements

The MERITE-HIPPOCAMPE cruise was organized and supported by the French Oceanographic Fleet (FOF), CNRS/INSU, IFREMER, IRD, the Tunisian Ministry of Agriculture, Water Resources and Fisheries and the Ministry of Higher Education and Scientific Research of Tunisia. We are grateful to the captains and crew of the R/V Antea for their help and assistance during the cruise, as well as the scientific crew for help in collecting and processing net samples on board. Zooplankton analyses were realized on the Microscopy and Imaging platform of MIO, which is partly funded by the European FEDER Fund (project no. 1166-39417).

Our thanks to all the participants involved in the MERITE HIPPOCAMPE project, in particular those taking part in the cruise and/or sharing constructive discussions: Sirine Amri, Malika Bel Hassen, Daniela Banaru, Sana Ben Ismail, Nagib Bhairy, Ismail Boudriga, Nicolas Briant, Sandrine Chifflet, Mohamed Nejib Daly Yahia, Thibault de Garidel-Thoroni, Karine Desboeufs, Boris Espinasse, Cédric Garnier, Catherine Guigue, Joel Knoery, Deny Malengros, Marouan Meddeb, Olivier Pringault, Marianne Quemeneur, Olivier Radakovitch, Christophe Ravel, Asma Sakka Hlaili, Cherif Sammari, Bastien Thomas, Javier Angel Tesán Onrubia, Jacek Tronczynski, Nourredine Zaaboub. We also acknowledge contributions of the reviewer and the associate editor for their constructive comments and suggestions.

Pamela Fierro González was supported by a Becas-Chile N°72190675 PhD scholarship by the National Agency for Research and Development (ANID), Government of Chile.

Appendix A. Supplementary data

Supplementary data to this article can be found online

References

Alcaraz, M., 1985. Vertical distribution of zooplankton biomass during summer stratification in the Western Mediterranean. In: Gibbs, P.E. (Ed.), Proceedings of the 19th European Marine Biology Symposium. Cambridge University Press, Cambridge, Plymouth, Devon, pp. 135–143.

Alcaraz, M., 1988. Summer zooplankton metabolism and its relation to primary production in the Western Mediterranean. In: Minas, H.J., Nival, P. (Eds.), Oceanographie Pelagique Mediterraneenne, Oceanologica Acta, 9, pp. 185–191.

Alcaraz, M., Calbet, A., Estrada, M., Marras, C., Saiz, E., Trepat, I., 2007. Physical control902 of zooplankton communities in the Catalan Sea. Prog. Oceanogr. 74 (2–3), 294–312. https://doi.org/10.1016/j.pocean.2007.04.003.

Alekseenko, E., Thouvenin, B., Tronczyński, J., Carlotti, F., Garreau, P., Tixier, C., Baklouti, M., 2018. Modeling of PCB trophic transfer in the Gulf of Lions; 3D coupled model application. Mar. Pollut. Bull. 128, 140–155. https://doi.org/10.1016/j.marpolbul.2018.01.008.

Alldredge, A., 1998. The carbon, nitrogen and mass content of marine snow as a function of aggregate size. Deep-Sea Res. I Oceanogr. Res. Pap. 45, 529–541. https://doi.org/10.1016/S0967-0637(97)00048-4.

Anderson, M.J., Gorley, R.N., Clarke, K.R., 2008. Guide to Software And Statistical Methods, p. 218.

Azam, F., Long, R.A., 2001. Sea snow microcosms. Nature 414, 495–498. https://doi.org/10.1038/35107174.

Bacosa, H.P., Kamalanathan, M., Cullen, J., Shi, D., Xu, C., Schwehr, K.A., Hala, D., Wade, T.L., Knap, A.H., Santschi, P.H., Quigg, A., 2020. Marine snow aggregates are enriched in polycyclic aromatic hydrocarbons (PAHs) in oil contaminated waters: insights from a mesocosm study. JMSE 8, 781. https://doi.org/10.3390/jmse8100781.

Battuello, M., Brizio, P., Mussat Sartor, R., Nurra, N., Pessani, D., Abete, M.C., Squadrone, S., 2016. Zooplankton from a North Western Mediterranean area as a model of metal transfer in a marine environment. Ecol. Indic. 66, 440–451. https://doi.org/10.1016/j.ecolind.2016.02.018.

Béjaoui, B., Ismail, S.B., Othmani, A., Hamida, O.B.A.-B.H., Chevalier, C., Feki-Sahnoun, W., Harzallah, A., Hamida, N.B.H., Bouaziz, R., Dahech, S., 2019. Synthesis review of the Gulf of Gabes (eastern Mediterranean Sea, Tunisia): morphological, climatic, physical oceanographic, biogeochemical and fisheries features. Estuar. Coast. Shelf Sci. 219, 395–408.

Bosse, A., Testor, P., Coppola, L., Bretel, P., Dausse, D., Durrieu de Madron, X., Houpert, L., Labaste, M., Legoff, H., Mortier, L., D'Ortenzio, F., 2022. LION observatory data. In: SEANOE. https://doi.org/10.17882/44411.

Bouloubassi, I., Méjanelle, L., Pete, R., Fillaux, J., Lorre, A., Point, V., 2006. PAH transport by sinking particles in the open Mediterranean Sea: a 1 year sediment trap study. Mar. Pollut. Bull. 52, 560–571. https://doi.org/10.1016/j.marpolbul.2005.10.003.

Briseño-Avena, C., Prairie, J.C., Franks, P.J.S., Jaffe, J.S., 2020. Comparing vertical distributions of Chl-a fluorescence, marine snow, and taxon-specific zooplankton in relation to density using high-resolution optical measurements. Front. Mar. Sci. 7, 602. https://doi.org/10.3389/fmars.2020.00602.

Castro-Jiménez, J., Bănaru, D., Chen, C.-T., Jiménez, B., Muñoz-Arnanz, J., Deviller, G., Sempéré, R., 2021. Persistent organic pollutants burden, trophic magnification and risk in a pelagic food web from coastal NW Mediterranean Sea. Environ. Sci. Technol. 55, 9557–9568. https://doi.org/10.1021/acs.est.1c00904.

Chifflet, S., Briant, N., Tesán-Onrubia, J.A., Zaaboub, N., Amri, S., Radakovitch, O., Bănaru, D., Tedetti, M., 2023. Distribution and accumulation of metals and metalloids in planktonic food webs of the Mediterranean Sea (MERITE-HIPPOCAMPE campaign). Mar. Pollut. Bull. 186, 114384 https://doi.org/10.1016/j.marpolbul.2022.114384.

Chouvelon, T., Strady, E., Harmelin-Vivien, M., Radakovitch, O., Brach-Papa, C., Crochet, S., Knoery, J., Rozuel, E., Thomas, B., Tronczynski, J., Chiffoleau, J.-F., 2019. Patterns of trace metal bioaccumulation and trophic transfer in a phytoplankton-zooplankton-small pelagic fish marine food web. Mar. Pollut. Bull. 146, 1013–1030. https://doi.org/10.1016/j.marpolbul.2019.07.047.

da Fonseca, E.M., Gaylarde, C., Baptista Neto, J.A., Camacho Chab, J.C., Ortega-Morales, O., 2022. Microbial interactions with particulate and floating pollutants in the oceans: a review. Micro 2, 257–276. https://doi.org/10.3390/micro2020017.

Das, K., Debacker, V., Pillet, S., Bouquegneau, J.M., 2002. Heavy metals in marine mammals. In: Toxicology of Marine Mammals, pp. 147–179.

Dolan, J.R., Marrasé, C., 1995. Planktonic ciliate distribution relative to a deep chlorophyll maximum: Catalan Sea, N.W. Mediterranean, June 1993. Deep-Sea Res. I Oceanogr. Res. Pap. 42, 1965–1987. https://doi.org/10.1016/0967-0637(95)00092-5.

Donoso, K., Carlotti, F., Pagano, M., Hunt, B.P.V., Escribano, R., Berline, L., 2017. Zooplankton community response to the winter 2013 deep convection process in the NW Mediterranean Sea: zooplankton and winter deep convection. J. Geophys. Res. Oceans 122, 2319–2338. https://doi.org/10.1002/2016JC012176.

Espinasse, B., Harmelin-Vivien, M., Tiano, M., Guilloux, L., Carlotti, F., 2014. Patterns of variations in C and N stable isotope ratios in size-fractionated zooplankton in the Gulf of Lion, NW Mediterranean Sea. J. Plankton Res. 36, 1204–1215. https://doi.org/10.1093/plankt/fbu043.

Feliú, G., Pagano, M., Hidalgo, P., Carlotti, F., 2020. Structure and function of epipelagic mesozooplankton and their response to dust deposition events during the spring PEACETIME cruise in the Mediterranean Sea. Biogeosciences 17, 5417–5441. https://doi.org/10.5194/bg-17-5417-2020.

Fenaux, R., 1968. Distribution verticale de la fréquence chez quelques Appendiculaires. Rapports et Procès-verbaux des Réunions, Commission Internationale pour l'Exploration Scientifique de la Mer Méditerranée, 19, pp. 513–515.

Fender, C.K., Kelly, T.B., Guidi, L., Ohman, M.D., Smith, M.C., Stukel, M.R., 2019. Investigating particle size-flux relationships and the biological pump across a range of plankton ecosystem states from coastal to oligotrophic. Front. Mar. Sci. 6, 603. https://doi.org/10.3389/fmars.2019.00603.

Foster, K.L., Stern, G.A., Pazerniuk, M.A., Hickie, B., Walkusz, W., Wang, F., Macdonald, R.W., 2012. Mercury biomagnification in marine zooplankton food webs in Hudson Bay. Environ. Sci. Technol. 46, 12952–12959. https://doi.org/10.1021/es303434p.

Gorsky, G., Dallot, S., Sardou, J., Fenaux, R., Carré, C., Palazzoli, I., 1988. C and N composition of some northwestern Mediterranean zooplankton and micronekton species. J. Exp. Mar. Biol. Ecol. 124, 133–144. https://doi.org/10.1016/0022-0981(88)90116-5.

Gorsky, G., Ohman, M.D., Picheral, M., Gasparini, S., Stemmann, L., Romagnan, J.-B., Cawood, A., Pesant, S., García-Comas, C., Prejger, F., 2010. Digital zooplankton image analysis using the ZooScan integrated system. J. Plankton Res. 32, 285–303. https://doi.org/10.1093/plankt/fbp124.

Granata, A., Bergamasco, A., Battaglia, P., Milisenda, G., Pansera, M., Bonanzinga, V., Arena, G., Andaloro, F., Giacobbe, S., Greco, S., Guglielmo, R., Spanò, N., Zagami, G., Guglielmo, L., 2020. Vertical distribution and diel migration of zooplankton and micronekton in Polcevera submarine canyon of the Ligurian mesopelagic zone (NW Mediterranean Sea). Prog. Oceanogr. 183, 102298 https://doi.org/10.1016/j.pocean.2020.102298.

Guglielmo, L., Minutoli, R., Bergamasco, A., Granata, A., Zagami, G., Antezana, T., 2011. Short-term changes in zooplankton community in Paso Ancho basin (Strait of Magellan): functional trophic structure and diel vertical migration. Polar Biol. 34, 1301–1317. https://doi.org/10.1007/s00300-011-1031-0.

Guieu, C., D'Ortenzio, F., Dulac, F., Taillandier, V., Doglioli, A., Petrenko, A., Barrillon, S., Mallet, M., Nabat, P., Desboeufs, K., 2020. Process studies at the air-sea interface after atmospheric deposition in the Mediterranean Sea: objectives and strategy of the PEACETIME oceanographic campaign (May–June 2017) (preprint). Biogeochem. Open Ocean. https://doi.org/10.5194/bg-2020-44.

Guigue, C., Tesán-Onrubia, J.A., Guyomarc'h, L., Bănaru, D., Carlotti, F., Pagano, M., Chifflet, S., Malengros, D., Chouba, L., Tronczynski, J., Tedetti, M., 2023. Hydrocarbons in size-fractionated plankton of the Mediterranean Sea (MERITE-HIPPOCAMPE campaign): concentrations and trophic transfer. Submitted, this special issue.

Khairy, M., Brault, E., Dickhut, R., Harding, K.C., Harkonen, T., Karlsson, O., Lehnert, K., Teilmann, J., Lohmann, R., 2021. Bioaccumulation of PCBs, OCPs and PBDEs in Marine Mammals From West Antarctica. Front. Mar. Sci. 8, 768715 https://doi.org/10.3389/fmars.2021.768715.

Kouwenberg, J.H.M., 1994. Copepod distribution in relation to seasonal hydrographics and spatial structure in the North-western Mediterranean (Golfe du Lion). Estuar. Coast. Shelf Sci. 38, 69–90. https://doi.org/10.1006/ecss.1994.1005.

Lehette, P., Hernández-León, S., 2009. Zooplankton biomass estimation from digitized images: a comparison between subtropical and Antarctic organisms: zooplankton biomass by digital images. Limnol. Oceanogr. Methods 7, 304–308. https://doi.org/10.4319/lom.2009.7.304.

Lombard, F., Boss, E., Waite, A.M., Vogt, M., Uitz, J., Stemmann, L., Sosik, H.M., Schulz, J., Romagnan, J.-B., Picheral, M., Pearlman, J., Ohman, M.D., Niehoff, B., Möller, K.O., Miloslavich, P., Lara-López, A., Kudela, R., Lopes, R.M., Kiko, R., Karp-Boss, L., Jaffe, J.S., Iversen, M.H., Irisson, J.-O., Fennel, K., Hauss, H., Guidi, L., Gorsky, G., Giering, S.L.C., Gaube, P., Gallager, S., Dubelaar, G., Cowen, R.K., Carlotti, F., Briseño-Avena, C., Berline, L., Benoit-Bird, K., Bax, N., Batten, S., Ayata, S.D., Artigas, L.F., Appeltans, W., 2019. Globally consistent quantitative observations of planktonic ecosystems. Front. Mar. Sci. 6, 196. https://doi.org/10.3389/fmars.2019.00196.

López-Urrutia, Á., Irigoien, X., Acuña, J., Harris, R., 2003. In situ feeding physiology and grazing impact of the appendicularian community in temperate waters. Mar. Ecol. Prog. Ser. 252, 125–141. https://doi.org/10.3354/meps252125.

Lovegrove, T., 1966. The determination of the dry weight of plankton and the effect of various factors on the values obtained. In: Some Contemporary Studies in Marine Science, pp. 407–420.

Margirier, F., Testor, P., Heslop, E., Mallil, K., Bosse, A., Houpert, L., Mortier, L., Bouin, M.-N., Coppola, L., D'Ortenzio, F., Durrieu de Madron, X., Mourre, B., Prieur, L., Raimbault, P., Taillandier, V., 2020. Abrupt warming and salinification of intermediate waters interplays with decline of deep convection in the Northwestern Mediterranean Sea. Sci. Rep. 10, 20923. https://doi.org/10.1038/s41598-020-77859-5.

Mazzocchi, M.G., Christou, E.D., Capua, I.D., Fernández de Puelles, M., Fonda-Umani, S., Molinero, J.C., Nival, P., Siokou-Frangou, I., 2007. Temporal variability of Centropages typicus in the Mediterranean Sea over seasonal-to-decadal scales. Prog. Oceanogr. 72, 214–232. https://doi.org/10.1016/j.pocean.2007.01.004.

Millot, C., Taupier-Letage, I., 2005. Circulation in the Mediterranean Sea. In: Saliot, A. (Ed.), The Mediterranean Sea, Handbook of Environmental Chemistry. Springer Berlin Heidelberg, Berlin, Heidelberg, pp. 29–66. https://doi.org/10.1007/b107143.

Möller, K., St John, M., Temming, A., Floeter, J., Sell, A., Herrmann, J., Möllmann, C., 2012. Marine snow, zooplankton and thin layers: indications of a trophic link from small-scale sampling with the Video Plankton Recorder. Mar. Ecol. Prog. Ser. 468, 57–69. https://doi.org/10.3354/meps09984.

Ndah, A.B., Meunier, C.L., Kirstein, I.V., Göbel, J., Rönn, L., Boersma, M., 2022. A systematic study of zooplankton-based indices of marine ecological change and water quality: application to the European marine strategy framework Directive (MSFD). Ecol. Indic. 135, 108587 https://doi.org/10.1016/j.ecolind.2022.108587.

Nowaczyk, A., Carlotti, F., Thibault-Botha, D., Pagano, M., 2011. Distribution of epipelagic metazooplankton across the Mediterranean Sea during the summer BOUM cruise. Biogeosciences 8, 2159–2177. https://doi.org/10.5194/bg-8-2159-2011.

Olivar, M.P., Emelianov, M., Villate, F., Uriarte, I., Maynou, F., Álvarez, I., Morote, E., 2010. The role of oceanographic conditions and plankton availability in larval fish assemblages off the Catalan coast (NW Mediterranean): larval fish assemblages off the Catalan coast. Fish. Oceanogr. 19, 209–229. https://doi.org/10.1111/j.1365-2419.2010.00538.x.

Paffenhöfer, G.-A., Stewart, T.B., Youngbluth, M.J., Bailey, T.G., 1991. High-resolution vertical profiles of pelagic tunicates. J. Plankton Res. 13, 971–981. https://doi.org/10.1093/plankt/13.5.971.

Riandey, V., Champalbert, G., Carlotti, F., Taupier-Letage, I., Thibault-Botha, D., 2005. Zooplankton distribution related to the hydrodynamic features in the Algerian Basin (western Mediterranean Sea) in summer 1997. Deep-Sea Res. I Oceanogr. Res. Pap. 52, 2029–2048. https://doi.org/10.1016/j.dsr.2005.06.004.

Romero, I.C., Sutton, T., Carr, B., Quintana-Rizzo, E., Ross, S.W., Hollander, D.J., Torres, J.J., 2018. Decadal assessment of polycyclic aromatic hydrocarbons in mesopelagic fishes from the Gulf of Mexico reveals exposure to oil-derived sources. Environ. Sci. Technol. 52, 10985–10996. https://doi.org/10.1021/acs.est.8b02243.

Rwawi, C., Hernandez-Carrasco, I., Tedetti, M., Rossi, V., 2023. Transport patterns and hydrodynamic context of the HIPPOCAMPE survey: implication for contaminant sources and distribution. In preparation for this special issue.

Sabatés, A., Salat, J., Palomera, I., Emelianov, M., Fernández De Puelles, M.L., Olivar, M. P., 2007. Advection of anchovy (Engraulis encrasicolus) larvae along the Catalan continental slope (NW Mediterranean). Fish. Oceanogr. 16, 130–141. https://doi.org/10.1111/j.1365-2419.2006.00416.x.

Sabatés, A., Zaragoza, N., Grau, C., Salat, J., 2008. Vertical distribution of early developmental stages in two coexisting clupeoid species, Sardinella aurita and Engraulis encrasicolus. Mar. Ecol. Prog. Ser. 364, 169–180. https://doi.org/10.3354/meps07461.

Saiz, E., Calbet, A., 2011. Copepod feeding in the ocean: scaling patterns, composition of their diet and the bias of estimates due to microzooplankton grazing during incubations. Hydrobiologia 666, 181–196. https://doi.org/10.1007/s10750-010-0421-6.

Saiz, E., Sabatés, A., Gili, J.-M., 2014. The zooplankton. In: Goffredo, S., Dubinsky, Z. (Eds.), The Mediterranean Sea. Springer Netherlands, Dordrecht, pp. 183–211. https://doi.org/10.1007/978-94-007-6704-1_11.

Sameoto, D., Wiebe, P., Runge, J., Postel, L., Dunn, J., Miller, C., Coombs, S., 2000. Collecting zooplankton. In: ICES Zooplankton Methodology Manual. Elsevier, pp. 55–81. https://doi.org/10.1016/B978-012327645-2/50004-9.

Sameoto, D.D., 1986. Influence of the biological and physical environment on the vertical distribution of mesozooplankton and micronekton in the eastern tropical Pacific. Mar. Biol. 93, 263–279. https://doi.org/10.1007/BF00508264.

Sieracki, C., Sieracki, M., Yentsch, C., 1998. An imaging-in-flow system for automated analysis of marine microplankton. Mar. Ecol. Prog. Ser. 168, 285–296. https://doi.org/10.3354/meps168285.

Siokou-Frangou, I., Christaki, U., Mazzocchi, M.G., Montresor, M., Ribera d'Alcalá, M., Vaqué, D., Zingone, A., 2010. Plankton in the open Mediterranean Sea: a review. Biogeosciences 7, 1543–1586. https://doi.org/10.5194/bg-7-1543-2010.

Strady, E., Harmelin-Vivien, M., Chiffoleau, J., Veron, A., Tronczynski, J., Radakovitch, O., 2015. 210Po and 210Pb trophic transfer within the phytoplankton–zooplankton–anchovy/sardine food web: a case study from the Gulf of Lion (NW Mediterranean Sea). J. Environ. Radioact. 143, 141–151. https://doi.org/10.1016/j.jenvrad.2015.02.019.

Tedetti, M., Tronczynski, J., Carlotti, F., Pagano, M., Sammari, C., Bel Hassen, M., Ben Ismail, S., Desboeufs, K., Poindron, C., Chifflet, S., Abdennadher, M., Amri, S., Bănarua, D., Ben Abdallah, L., Bhairy, N., Boudriga, I., Bourin, A., Brach-Papa, C., Briant, N., Cabrol, L., Chevalier, C., Chouba, L., Coudray, S., Daly Yahia, M.N., de Garidel-Thoron, T., Dufour, A., Dutay, J.-C., Espinasse, B., Fierro-González, P., Fornier, M., Garcia, N., Giner, F., Guigue, C., Guilloux, L., Hamza, A., Heimbürger-Boavida, L.-E., Jacquet, S., Knoery, J., Lajnef, R., Makhlouf Belkahia, N., Malengros, D., Martinot, P.L., Bosse, A., Mazur, J.-C., Meddeb, M., Misson, B., Pringault, O., Quéméneur, M., Radakovitch, O., Raimbault, P., Ravel, C., Rossi, V., Rwawi, C., Sakka Hlaili, A., Tesán Onrubia, J.A., Thomas, B., Thyssen, M., Zaaboub, N., Zouari, A., Garnier, C., 2023. Contamination of planktonic food webs in the Mediterranean Sea: setting the frame for the MERITE-HIPPOCAMPE oceanographic cruise (spring 2019). Mar. Pollut. Bull. 189, 114765 https://doi.org/10.1016/j.marpolbul.2023.114765.

Tesán-Onrubia, J.A., Tedetti, M., Carlotti, F., Tenaille, M., Guilloux, L., Pagano, M., Lebreton, B., Guillou, G., Fierro-González, P., Guigue, C., Chifflet, S., Garcia, T., Boudriga, I., Belhassen, M., Bellaaj-Zouari, M., Bănaru, D., 2023. Spatial variations of biochemical content and stable isotope ratios of size-fractionated plankton in the Mediterranean Sea (MERITE-HIPPOCAMPE campaign). Mar. Pollut. Bull. 189, 114787 https://doi.org/10.1016/j.marpolbul.2023.114787.

Tiano, M., Tronczyński, J., Harmelin-Vivien, M., Tixier, C., Carlotti, F., 2014. PCB concentrations in plankton size classes, a temporal study in Marseille Bay, Western Mediterranean Sea. Mar. Pollut. Bull. 89, 331–339. https://doi.org/10.1016/j.marpolbul.2014.09.040.

Tiselius, P., Petersen, J., Nielsen, T., Maar, M., Møller, E., Satapoomin, S., Tönnesson, K., Zervoudaki, T., Christou, E., Giannakourou, A., Sell, A., Vargas, C., 2003. Functional response of Oikopleura dioica to house clogging due to exposure to algae of different sizes. Mar. Biol. 142, 253–261. https://doi.org/10.1007/s00227-002-0961-z.

Van der Oost, R., Beyer, J., Vermeulen, N.P.E., 2003. Fish bioaccumulation and biomarkers in environmental risk assessment: a review. Environ. Toxicol. Pharmacol. 13, 57–149. https://doi.org/10.1016/S1382-6689(02)00126-6.

Weijs, L., Hickie, B., Blust, R., Covaci, A., 2014. Overview of the current state-of-the-art for bioaccumulation models in marine mammals. Toxics 2, 226–246. https://doi.org/10.3390/toxics2020226.

Wen, L.-S., Lee, C.-P., Lee, W.-H., Chuang, A., 2018. An ultra-clean multilayer apparatus for collecting size fractionated marine plankton and suspended particles. JoVE 56811. https://doi.org/10.3791/56811.